Second-day road log, from Alamogordo to Tularosa, Rhodes Canyon, Lake Lucero, and return to Alamogordo

Katherine A. Giles, Spencer G. Lucas, Virgil W. Lueth, and Robert G. Myers
2002, pp. 29-51. https://doi.org/10.56577/FFC-53.29

in:

Geology of White Sands, Lueth, Virgil; Giles, Katherine A.; Lucas, Spencer G.; Kues, Barry S.; Myers, Robert G.; Ulmer-Scholle, Dana; [eds.], New Mexico Geological Society 53rd Annual Fall Field Conference Guidebook, 362 p. https://doi.org/10.56577/FFC-53

This page is intentionally left blank to maintain order of facing pages.

SECOND-DAY ROAD LOG, FROM ALAMOGORDO TO TULAROSA, RHODES CANYON, LAKE LUCERO, AND RETURN TO ALAMOGORDO

KATHERINE A. GILES, SPENCER G. LUCAS, VIRGIL W. LUETH,
AND ROBERT G. MYERS

Assembly Point: Holiday Inn Express, Alamogordo
Departure time: 7:45 AM
Distance: 106.7 miles
Stops: 6

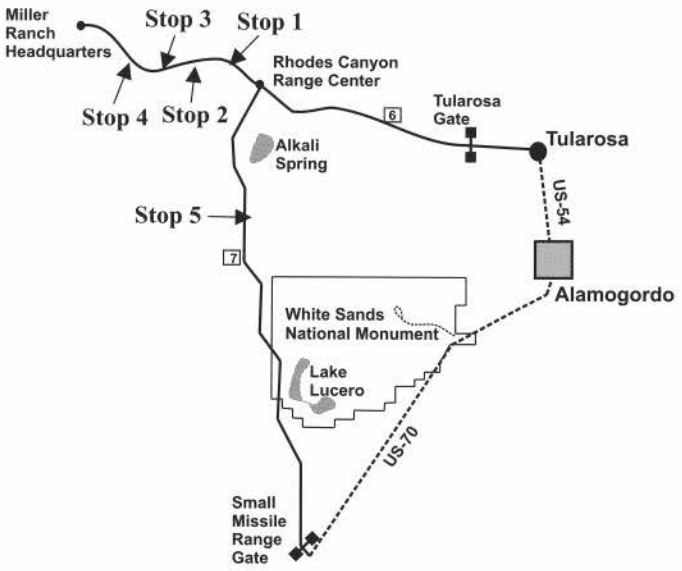

SUMMARY

Today's trip examines the classic section of Paleozoic strata exposed in the San Andres Mountains and Pleistocene-Recent basin-floor lacustrine and eolian deposits of the Tularosa Basin. The trip begins by retracing yesterday's route north to Tularosa and then west to enter the White Sands Missile Range via the Tularosa gate on Range Road 6. Then, instead of heading north to the Carrizozo lava flows along Range Road 9, we proceed due west across the floor of the Tularosa Basin on Range Road 6 to the eastern flank of the San Andres Mountains at Rhodes Canyon.

The drive westward through Rhodes Canyon allows us to examine, in ascending stratigraphic order, more than 7000 ft of Paleozoic strata. Stops feature outcrops of Proterozoic, Cambrian, Ordovician, Pennsylvanian and Permian rocks. A stop at the Bear Den Canyon fault also allows us to examine a portion of the Devonian-Mississippian section and problems of local structure. The tour culminates at Rhodes Pass, where we turn around and retrace our route eastward to the floor of the Tularosa Basin.

The trip then proceeds south, driving along the western edge of Alkali Flat and Lake Lucero, remnants of the Late Pleistocene Lake Otero, which once inundated an estimated 700 mi^2 of the Tularosa Basin floor. Our last stop examines sediments of Lake Otero and mammoth tracks impressed near its paleo-shoreline.

0.0/106.7 This is **mile 22.1 of the First-day roadlog**. Intersection of paved roads, Range Road 6 and Range Road 9; **go straight** (west) on Range Road 6; Note Tularosa Peak to south at 9:00. The basin actually consists of two half grabens, the shallower of the two is on the east side of the basin (Seager et al., 1987). Darton (1928) produced a cross-section of the basin along the line we are travelling (Fig. 2.1). The Jarilla fault is located

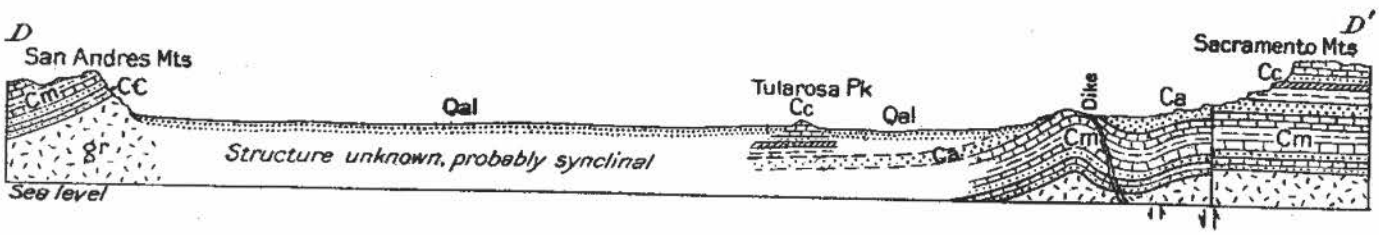

FIGURE 2.1. Cross-section of the Tularosa Basin as presented by Darton (1928). The basin consists of two half-grabens separated by the Jarilla Fault zone. The location of the fault zone is immediately west of Tularosa Mountain in the area labeled, "Structure unknown, probably synclinal."

just west of Tularosa Peak in the area where Darton labeled the cross section, "Structure unknown, probably synclinal." The road is now traversing a thin veneer of very young, non-gypsiferous dunes on the less down-dropped, east half graben. **(1.9)**

1.9/104.8 Tula-G launch site to left, and Brazel Lake to right. Brazel Lake marks the terminus of Tularosa Creek. The lake level varies significantly due to runoff conditions in the Tularosa Creek drainage basin. **(0.3)**

2.2/104.5 Note calcified soil development on dunes to the right. **(0.5)**

2.7/104.0 Gypsum dune fields for the next 2 miles. **(0.6)**

3.3/103.4 Road curves right, note White Sands in distance to left. **(2.0)**

5.3/101.4 Road curves right. **(0.7)**

6.0/100.7 Road curves left. **(0.1)**

6.1/100.6 Small playas (note one on the south side of the road) dot the dune fields locally. **(1.0)**

7.1/99.6 Road curves right. Small playa to north is Fifteenmile Lake. **(0.3)**

7.4/99.3 Road to left. **(0.8)**

8.2/98.5 Road curves toward south. **(0.6)**

8.8/97.9 Road curves toward south. Cottonwood Canyon in the San Andres Mountains is dead ahead. **(2.3)**

11.1/95.6 Paved road to left, then paved road to right. **(0.6)**

11.7/95.0 Road curves right, note roadcut in non-gypsum dune on north side of road. **(1.0)**

12.7/94.0 Road curves right **(0.2)**

12.9/93.8 Roads to right and left. **(0.4)**

13.3/93.4 Road curves toward south, view to south of Big Salt Lake playa. **(0.9)**

14.2/92.5 Road curves toward north, playa to south. **(0.5)**

14.7/92.0 Road drops down to enter playa lake. **(0.1)**

14.8/91.9 Cross bridge over Salt Creek **(1.0)**

15.8/90.9 Road climbs up over playa edge. **(1.3)**

17.7/89.0 Road on left; road curves right. **(1.7)**

19.4/87.3 Crest of hill, road to right to NATO missile test center. Good Fortune Canyon at 12:00. (Fig. 2.2) **(2.2)**

FORGOTTEN BY MOST – REMEMBERED BY A FEW, THE GOOD FORTUNE CAMP, SAN ANDRES MOUNTAINS, SIERRA COUNTY, NEW MEXICO

Robert W. Eveleth

New Mexico Bureau of Geology and Mineral Resources, 801 Leroy Place, Socorro, NM 87801, ginger@gis.nmt.edu

Good Fortune Camp in the San Andres Mountains of south-central New Mexico, once one of the more promising and busy mining camps in Socorro County, is forgotten by all but a few today. The area has been included within the boundaries of the White Sands Missile Range (WSMR) since 1945 and is currently off limits to the civilian traveler. Two principal periods of activity date from discovery in ca. 1881 to about 1910 and from 1925 to 1945. No patented mining claims exist in the San Andres mining district. Locations under the general mining law have been abandoned and restaked under a plethora of names by each successive generation of prospectors. Little remains of the camp, although it was once home to dozens of miners and their families as the stone foundations and ruins attest (Jim Eckles, pers. comm., 2001). The author visited with Mrs. Ruth Kruse Adams, daughter of Juanita Andrace Friend (Kruse), the first child born in Good Fortune Camp on February 6, 1894. Her father, John K., and her Uncle Lewis Friend located the first mining claims in the district three years before. Mrs. Kruse often recalled the primitive conditions then existing in camp — the nearest supplies and medical facilities lay a full day's journey across the Jornada del Muerto at Fort Craig. Mrs. Kruse attained the venerable age of 101 – an achievement that may reflect the magical qualities of the Good Fortune spring waters or the Fort Craig medical facilities – or both (Eveleth, 1984, 2001)!

The range is an uplifted block of Precambrian rock whose eastern slopes are dominated by pinkish granite overlain by Paleozoic sediments, the most prominent of which are the Lead Camp Limestone and the Panther Seep Formation. These two sedimentary units are host rocks to ore deposits in the district. These strata are intruded by the Salinas Peak laccolith. Productive ore bodies have been found exclusively where the limestones are in contact with the Salinas Peak laccolith or more rarely the Precambrian granite (Bachman and Harbour, 1970; Lasky, 1932).

Many deposits in the San Andres mining district are associated with major faults trending northwest-southeast and traceable for

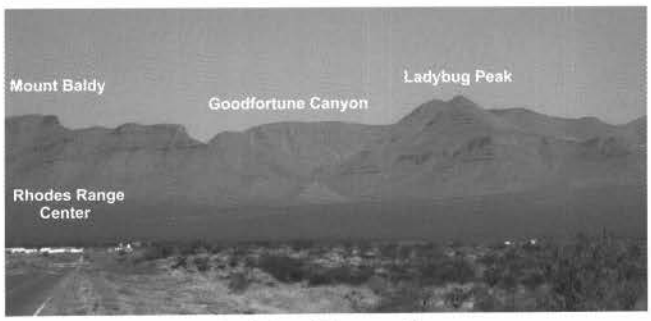

FIGURE 2.2. Photograph of Good Fortune Canyon.

miles in Good Fortune Canyon. Others north and east of Salinas Peak are found along the depositional contacts. Principal ore minerals include galena sphalerite, chalcopyrite, pyrite, chalcocite, malachite, and azurite. The major gangue minerals included hematite, quartz, calcite, barite, and fluorite (Lasky, 1932). Gold, almost totally absent in the lead ores, is a sparse constituent in the copper veins and was sufficiently abundant at the Blackington prospect to be visible in hand specimens (Leeson, 1896). Extant production records indicate that the lead zones were remarkably free from copper and vice-versa and that the ore minerals were highly concentrated in narrow veins (except in the Salinas Peak area) and often graded well over 30% of each metal (NM Bureau of Geology Archives). Deposits of this grade are what attracted prospectors – both American and earlier the Spanish— to the area (Leeson, 1896).

One of the first American prospectors to arrive in the region in ca. 1879 was the accomplished and highly regarded Civil War Indian Scout, Captain Jack Crawford, who was repeatedly credited with routing out the Indians and making the area safe for the prospectors that followed him (Bullion, 5/1/1883, p 3; 12/1/1884, p 5). Crawford established base camps for his prospecting activities – and Good Fortune Camp was one of them (Bullion 12/1/1884, p 5; Prince Papers). Other pioneer prospectors following Crawford into the San Andres included the Friend Brothers, Thomas Holland and James Cole, who collectively located the first claims in the district. A second generation included men like L. Bradford Prince, Eugene Manlove Rhodes, Dr. Charles F. Blackington, John R., DeMeier, and dozens of others.

The Friend Brothers located the Good Fortune, Grand Mogul, and Alton lodes by May 1881 and within a year (some 100 claims had been filed (Socorro County, Book 1, p 344; Book 3, p 308; Gazetteer, 1992, p 157). Local miners formally established the San Andres mining district bounded on the south by Antelope Canyon (Mackinson Canyon?), west by the Jornada, and east by the Gypsum Plains (Socorro County, Book 4, p 456). And on the north? Well, they accidentally omitted that one – a later mining journal article defined it as the Fort Stanton Road. The "Fort Stanton Road" was the old government road through Thurgood Canyon (variously misspelled as Thoroughgood, Thrugood, etc.) north of Salinas Peak and which derives from rancher Eugene E. Thurgood, who homesteaded the area around Dripping Springs (Fig. 2.3) near the turn of the century (*Chieftain*, 6/13/1908, p 4).

The region buzzed with mining and exploration activity for the first decade or two with hundreds of claims being located and developed. The Friend Brothers added many additional to their first three; L. Bradford Prince held a dozen or so copper claims, and Crawford ultimately staked four dozen between Good Fortune Camp and Johnson Park Canyon. Despite their labors, the early prospectors developed few significant ore bodies and by 1890, most of them — except for Captain Jack — had moved on to greener pastures. By 1887, Crawford had invested some $15,000 of his own funds in his properties. Before heading east for one of his many theatrical tours he told the editor of the Bullion "I came to New Mexico to stay, and it is probable that my bones will rest here, and if my expectations are half realized I shall put many a thousand more into and on top of the ground."

FIGURE 2.3. Ruins of Good Fortune Camp. Photo courtesy of Jim Eckles.

Throughout the 1890s he was still performing assessment work and sending out occasional ore shipments (Bullion, 3/5/1887, p 1; 2//9/1892, p 7; Socorro County, Book 44, p 326)."

Socorro old-timer J. J. Leeson, President of the New Mexico Immigration Bureau, whose personal hobby was collecting New Mexico minerals and mining lore, recorded the story of the Spanish mine. Local prospectors searched for the alleged mine in the San Andres for at least twenty years. The deposit "was discovered in 1655 by one of the followers (possibly Marguerito Luero) of that noted priest, missionary, and explorer, Father Guerra, and was recorded in the town of Franklin, which is now El Paso, Texas" (Leeson, 1896, p 43). The Spanish miners constructed a stone cabin complete with shot-holes, in which they took refuge when attacked by the Indians – which was probably often. They managed to ship out some rich ore but were ultimately forced out of the area.

Dr. Charles F. Blackington, another Socorro resident, was the lucky re-discoverer – perhaps the ruins of the cabin caught his eye – and in 1895, he immediately staked nine lode mining claims over the deposit (Socorro County, Book 14, p 736). The mine is located about four miles southeast of Good Fortune Spring along one of the major faults on the east side of the canyon and, it should be noted, is identical to Lasky's "Blackendon" prospect (Lasky, 1932, p 79). Blackington shipped out several lots of high-grade copper ore through about 1900. Native gold was said to be visible in hand specimens, and the metal contributed significantly to the value of the shipments (Leeson, p 44; International Industrial Record, p 45). Other well developed properties active at the time included the Tipton Copper Company's workings in Good Fortune Canyon (Tipton Spring area?), and the Lead King and Queen prospects near Salinas Peak. The Columbia Copper Co. was shipping small lots of high-grade copper ore by 1908, and two years later J. S. Lavern produced a final lot from the Good Fortune mine (both the above doubtless Blackington's prospect), closing the door on activity for about 15 years (Southwestern Opportunities, no page cited; Min. Res., 1910, p 552).

The miners returned in ca. 1925 but focused their attention on deposits in the extreme southeastern and northern portions of the

district. NMBM&MR geologist Sam Lasky visited in 1929 but examined only the elusive Bella Vista prospect (which fell upon Sam's Yankee ears as "Valle Vista") about a mile south of the mouth of Good Fortune Canyon (Lasky, p 77-80). The Bella Vista is one of those few deposits found at the contact between the Precambrian and the Paleozoic sediments, and some of the best ore was found in the granite. Small lots of very high-grade copper ore were produced by the miners through 1939 (Min. Res., 1939, p 432). Other mines worked at this time were variously known as the Salinas Mine, Nighthawk Group, and Crawford prospect (Lasky, p 82) and were doubtless part of Crawford's southernmost claim group. The properties produced high-grade lead-zinc shipments until the area was withdrawn by WSMR (Min. Res., 1948, p 1578). Several investigators have speculated that if the mineralization is continuous between the Salinas mine and the group of prospects about a mile northeast (and there is some geologic evidence to support this premise), this could have developed into a lead-zinc-barite-fluorite deposit of a size and grade sufficient to sustain an economic mining operation. Such would be an appropriate and lasting monument to the pioneer prospector and developer, Captain Jack Crawford, the man who initially made the area safe for prospectors and probably invested more funds, labor, and time in the district than any other individual.

History often forgets the prospectors and miners who originally opened up a district, and the Good Fortune Camp pioneers are no exception. Just for the record, Captain Jack went on to fame and fortune with his many collections of prose, poetry, and song. The Friend Brothers migrated to the gold camps of Arizona and Mexico but left their mark in the area: the "Little Louella" patented mining claim at Kelly is named for their oldest daughter and their youngest daughter Juanita, the first child born in camp, was named for Col. E. W. Eaton's mine at Kelly. Eugene Manlove Rhodes quickly turned his back on a mining career and instead staked his claim in the rich lode of cowboy lore, turning out many classic western novels. Bradford Prince became territorial governor of New Mexico, and Charles Blackington served four exemplary years as Socorro County sheriff and partook in some of the most spectacular crimes of his day. And, what of John R. DeMier? DeMier's prospector's "nose" ultimately led him to something more lucrative than the San Andres copper mines: the extensive guano deposits in Bat Cave near Lava Station. DeMier developed lucrative markets for the product, eventually sold his operation to a group of California investors, and retired a moderately wealthy man. Which clearly serves to prove "all that glitters is not gold!"

21.6/85.1 Stop sign; road intersection of Range Road 6 with Range Road 7 at Rhodes Canyon Range Center; **go straight** ahead (west) on road up to Rhodes Canyon. **(0.9)**

22.5/84.2 Road curves left; Rhodes Canyon at 12:00, Salinas Peak at 1:00 and Sheep Mountain at 2:00. **(0.3)**

23.8/82.9 Road curves right; note the Paleozoic section exposed ahead on the eastern flank of the San Andres Mountains (Fig, 2.4). This is the lower part of the section we will be examining closely today. The upper part of the section we will view long distance from Miller Ranch in the strike valley in the center of the range. (Fig. 2.5).

Above the reddish Precambrian granite note a thin black band—the Cambrian Bliss Formation, here about 50 ft of mostly quartzose sandstone. The recessed slope above the Bliss is about 360 ft thick and is formed by ledgy dolostone and limestone of the Ordovician El Paso Formation. The overlying prominent dark cliff is about 260-ft thick and composed mostly of dolostone of the Ordovician Montoya Formation. The Silurian Fusselman Dolomite overlies the Montoya to the south but is not present in Rhodes Canyon due to major erosion in the late Silurian or Early Devonian. The Montoya in Rhodes Canyon is overlain by slope-forming Devonian strata comprising thin-bedded limestone, siltstone and shale of the Oñate Formation (32 ft) overlain by siltstone and shale of the Sly Gap Formation (31 ft) and capped by shale of the Contadero Formation (75 ft). The Mississippian Lake Valley Formation (about 60 ft of limestone-dominated strata) forms the first thin cliffs above the slope-forming Devonian strata. The prominent cliff on the skyline is the lower Pennsylvanian Lead Camp Limestone, which is about 850 ft thick here. **(0.5)**

24.3/82.4 Road curves left, then right (S-curve) and continues in this manner for about 1 mile. **(1.4)**

25.7/81.0 Guard house on left for USAF Ram Site, pavement ends; continue straight on unpaved road. **(1.5)**

27.2/79.5 Road curves right; note section ahead on Amole Ridge of Proterozoic granite through Middle Pennsylvanian limestone. **(1.5)**

27.8/78.9 Road to left provides access to radar station. Strata behind the station are faulted down to the east. **(0.3)**

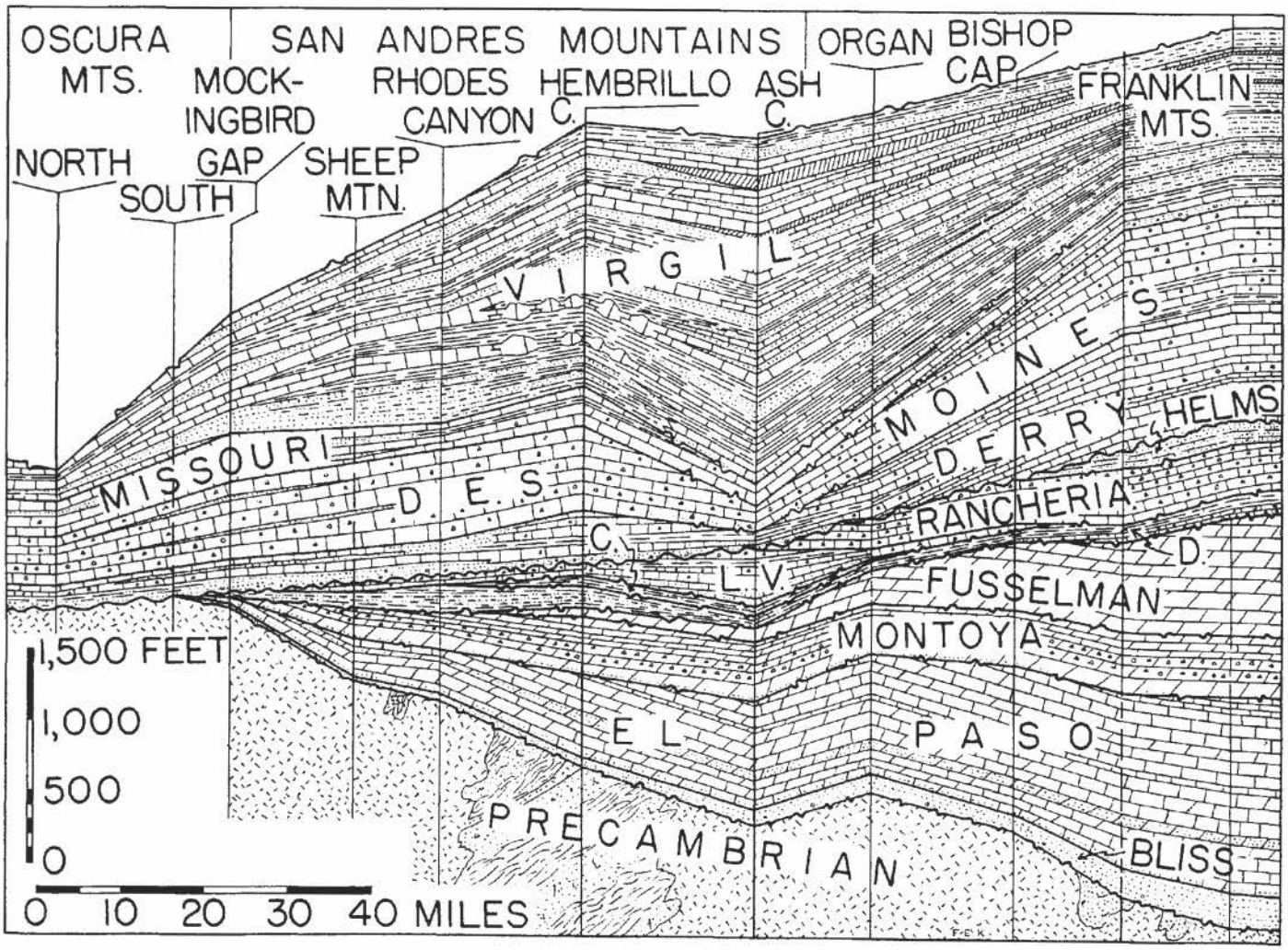

FIGURE 2.4. Stratigraphy of the middle portion of the San Andres Range (from Kottlowski and LeMone, 1994).

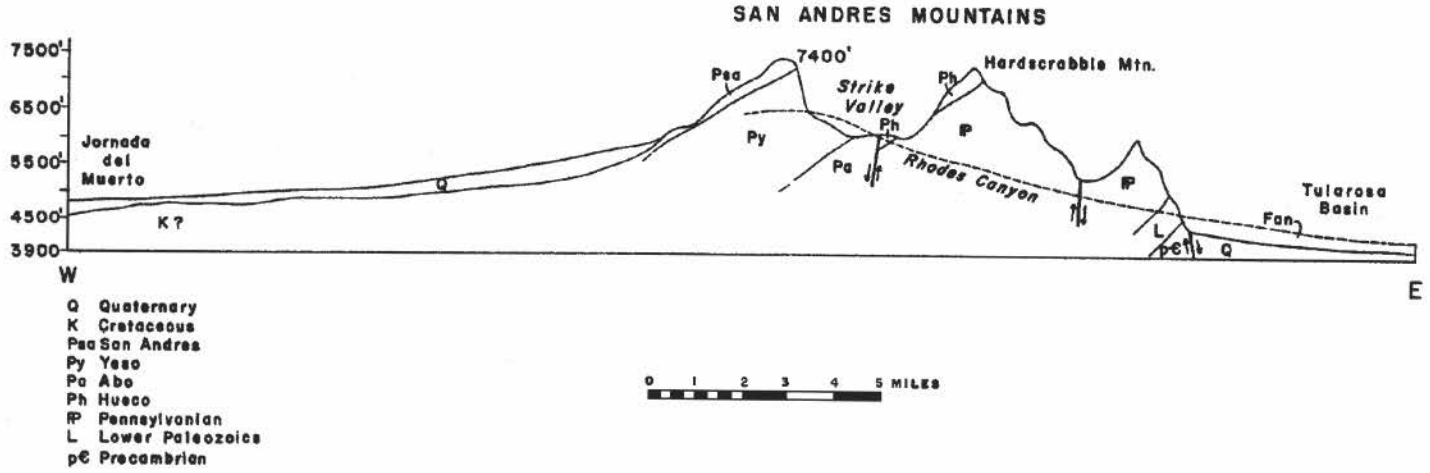

FIGURE 2.5. Topographic profile and structure section of the San Andres in the Rhodes Canyon area (after Kottlowski, et al., 1955).

28.1/78.6 Road to right; **continue straight**. We are driving up the Rhodes Canyon fan described by Hawley (1983). The fan is mostly made up of coarse-grained piedmont slope deposits of probable early to middle Pleistocene age. These are boulder-to-pebble gravels mostly of limestone and dolomite clasts in a calcareous sandy loan matrix. **(0.5)**

28.6/78.1 Road curves right. Good view up Seep Canyon reveals two cliffs of limestone, the lower Ordovician and the upper Middle Pennsylvanian. Note the prominent but thin black band below them – the Cambrian Bliss Formation (Fig. 2.6) **(0.3)**

28.9/77.8 Outcrop on left is fault block of Montoya Group. **(0.8)**

29.7/77.0 Tip Top Canyon to south. **(0.6)**

30.3/76.4 **STOP 1.** Road cut of Cambro-Ordovician Bliss Formation on the right (north), side of the road. We will climb up section in the first small drainage to the east of the road cut on the northern side of the road (Fig. 2.7). Here, we will examine the contact of the Bliss Formation with Precambrian granite, the gradational upper contact of the Bliss with the overlying carbonate strata of the El Paso Formation, and the Montoya Formation.

The Bliss Formation represents transgressive sandstone deposition over a highly eroded Precambrian surface. The Bliss thins northward from 250 ft in the Franklin Mountains to a depositional pinchout near the Sierra-Socorro county line (Kottlowski, 1963). In Rhodes Canyon, the measured thickness varies from 6 ft (Darton, 1928) to 80 ft (Kelley and Silver, 1952). Kottlowski et al. (1956) record 46 ft. The reported thickness variation is derived from the difficulty in choosing the upper contact of the Bliss with the El Paso Formation, which is a gradational contact. Kelley and Silver (1952) based their contact on changes in color, topographic expression, and locally a discomformity. Kottlowski et al (1956) used the change in color from dark-weathering glauconitic and hematitic sandstone (Bliss) to light-colored ledgy arenaceous carbonate (El Paso Formation). The basal few feet of the Bliss comprises cross-bedded, bioturbated, coarse-grained arkosic sandstone and granite pebble to cobble conglomerate. The basal unit is overlain by a few feet of oolitic ironstone (see Mack minipaper for discussion) and fine-grained glauconitic sandstone and siltstone that grade abruptly upward into quartzose sandstone interbedded with limestone and dolostone. The overlying El Paso Formation is about 300 ft thick here and forms a steep ledgy slope of interbedded light gray subtidal lime-

FIGURE 2.6. Photograph of Seep Canyon with lower cliff forming units of lower Ordovician age and upper cliffs composed of Middle Pennsylvanian rocks.

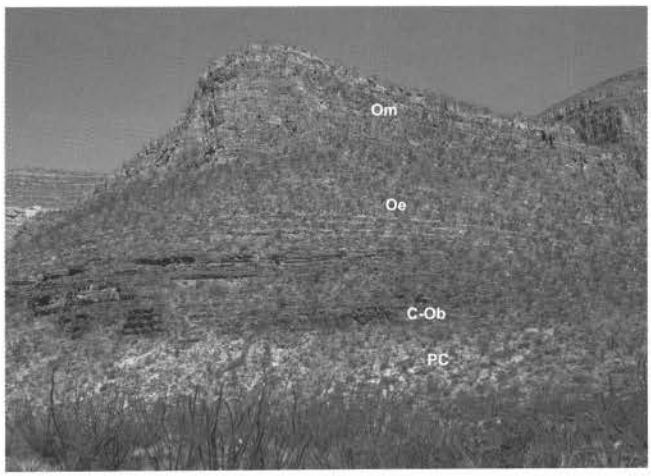

FIGURE 2.7. Small hill of lower Paleozoic rock units. Basal Bliss Sandstone consists of arkosic sandstones and conglomerates with a thin interval of oolitic ironstone rests on Proterozoic granite. Interbedded limestone and dolostone of the El Paso Formation conformably overlies the Bliss forming the steep ledgy slopes. Montoya Dolomite caps the hill.

stone and light brown peritidal dolostone with rare thin sandstone beds (see Pope minipaper for discussion of facies present in the El Paso and Montoya formations). Note, we employ the term El Paso Formation here instead of El Paso Group, which is used in the Franklin Mountains to the south, because the internal "formations" recognized and mapable in the Franklin Mountains are either not present or are not mapable in Rhodes Canyon, The contact between the El Paso Formation and the overlying Cable Canyon Sandstone Member of the Montoya Formation is a sharp disconformity. The Cable Canyon Sandstone consists of 25 ft of conglomeratic quartzose sandstone and grades upward into massive, cherty, crinoidal dolostone beds of the Upham Dolomite Member. **(0.4)**

ENIGMATIC OOLITIC IRONSTONE IN THE CAMBRO-ORDOVICIAN BLISS SANDSTONE

Greg H. Mack
Department of Geological Sciences, New Mexico State University, Las Cruces, New Mexico 88003; gmack@nmsu.edu

The basal Paleozoic sedimentary unit in south-central New Mexico is the Bliss Sandstone. Scattered fossils in the Bliss suggest an age from late Cambrian (Franconian and Trempealeauan) to earliest Ordovician (early Gasconadian) (Flower, 1969; Repetski, 1988; Taylor and Repteski, 1995). The Bliss consists primarily of brown and maroon, coarse- to very fine-grained sandstone and siltstone, often glauconitic, and local interbeds of limestone and dolostone. Approximately 75 m thick in the southern Franklin Mountains near El Paso, Texas, the Bliss thins northward in south-central New Mexico to a depositional zero edge near the Sierra-Socorro county line (Kottlowski, 1963).

An unusual rock type in the Bliss is oolitic ironstone, which was first recognized by Herrick (1899) and subsequently described on a regional scale by Kelley (1949, 1951). As defined by Kelley (1951), the stratigraphic interval of oolitic ironstone in the Bliss ranges from 0.2 to 2.5 m thick and occupies an east-trending belt approximately 30 km wide from just north of Silver City, through the Black Range and Caballo Mountains, to the northern San Andres Mountains. Oolitic ironstone beds in the Bliss were subsequently found in the southern San Andres Mountains by Kottlowski et al. (1956) and at San Diego Mountain by the author, enlarging the width of the belt by about 15 km to the south. The oolitic ironstone interval either occupies the base of the Bliss or is several meters above the base in a stratigraphic position between cross-bedded, *Skolithos*-bearing medium- to coarse-grained sandstone below and thin-bedded, very fine-grained, glauconitic sandstone and siltstone above. Ooids in the Bliss range in size from very fine sand to granule, generally consist of a nucleus of detrital quartz surrounded by laminae of hematite and minor chlorite (chamosite?), and are cemented by hematite, quartz, chalcedony, and/or carbonate (Kelley, 1951).

The origin of Phanerozoic oolitic ironstones is controversial. It is generally accepted that the original iron-bearing mineral in the ooids was either berthierine (iron-rich serpentine) or goethite, although exactly how and in what environment the ooids form is a matter of debate (Young, 1989). Alteration of berthierine to chamosite (iron-rich chlorite), goethite, hematite, siderite, or pyrite may occur during diagenesis (Young, 1989).

There are three models for the origin of oolitic ironstones. One model involves the creation of goethite ooids and pisoliths in ferruginous soils, such as tropical laterites, and their subsequent reworking into fluvial, lacustrine, or shallow-marine environments (Siehl and Thein, 1989). In a second model, berthierine ooids precipitate at the sediment-seawater interface in lagoonal or open-shelf environments characterized by slow sediment accumulation rates. In this model, the iron is supplied to the sea via terrestrial weathering presumably associated with humid, tropical climates (Young, 1989). The exhalative model also involves precipitation of berthierine ooids at the sediment-seawater interface, but the iron is supplied to the sea by fluids moving upward from crustal sources through faults or fractures. The exhalative model is based on the formation of modern iron ooids off the coast of Mala Pascua, Venezuela, and there is some disagreement as to whether the fluids are deep-seated igneous fluids or seawater recycled through the oceanic crust (Kimberley, 1994). It is not yet clear whether the oolitic ironstone in the Bliss conforms to one of these models or has another origin.

EARLY ORDOVICIAN EL PASO FORMATION AND LATE ORDOVICIAN MONTOYA FORMATION, RHODES CANYON

Michael Pope
Department of Geology, Washington State University, Pullman, WA 99164, mcpope@wsu.edu

The Late Cambrian to Early Ordovician El Paso Formation and unconformably overlying Late Ordovician Montoya Formation are well exposed in Rhodes Canyon. These units were deposited on a gently sloping passive margin that faced a vast open ocean to the south. The El Paso Formation conformably overlies the Late Cambrian-Early Ordovician Bliss Sandstone and consists regionally of 100's to 1000's of feet of interbedded limestone, dolomite and rare sandstone deposited during global greenhouse conditions. A disconformity representing an ~30 Ma hiatus separates the El Paso Formation from the Montoya Formation. A basal sandstone in the Montoya Formation grades

conformably upward into fossiliferous dolomite, cherty dolomite and massive dolomudstone. The Montoya Formation was deposited during a transition to global glaciation that occurred during the Late Ordovician. The Montoya Formation is unconformably overlain by the Late Early Silurian Fusselman Dolomite or the Middle to Late Devonian Percha Shale.

The El Paso Formation is a mixed carbonate and sandstone unit ~306 feet thick in Rhodes Canyon that begins at the top of the Bliss Sandstone. It is easily distinguished regionally because it commonly consists of thick, interbedded packages of gray, subtidal limestone and yellow-tan peritidal dolomite with rare, thin sandstone interbeds. The subtidal limestone commonly contains domal sponge-stromatolite bioherms, extensive burrowing, ooids, oncoids, and trilobite fragments. Conversely, the peritidal dolomite commonly is devoid of skeletal fragments and contains cryptalgal laminites, mudcracks, teepee structures, evaporite pseudomorphs, voids or chert nodules after evaporites, and some thin sandstone interbeds. The sandstone commonly is cross-bedded and glauconitic. These facies commonly are stacked into disconformably-bounded, meter-scale units with average cycle durations of 20-100 ky that likely formed by sea level changes produced by Milankovitch climate forcing mechanisms (Goldhammer et al., 1993). Similar age units, with very similar internal cycle characteristics can be found in Texas, Oklahoma, the Appalachian Basin and throughout the Great Basin (Goldhammer et al., 1993; Read and Goldhammer, 1988). The larger, 10's to 100's of feet thick units of limestone and dolomite reflect longer term (1-5 Ma), likely tectonically driven, changes in accommodation space on the passive margin (Goldhammer et al., 1993). The El Paso Formation is equivalent to the subsurface Ellenburger Formation that is an important gas reservoir in Texas and southeastern New Mexico. Much of the gas in this reservoir is contained in the extensive cave system that formed during the development of the regional unconformity between the El Paso Formation and overlying Montoya Formation.

The Montoya Formation represents a single long-term (10-15 Ma duration) transgression and regression of sea level onto the passive margin. The Montoya Formation is subdivided into four distinct members, in ascending order, the Cable Canyon Sandstone, Upham Dolomite, Aleman Dolomite and Cutter Dolomite. The Cable Canyon Sandstone is the lowest part of the Montoya Formation and occurs only in the northern part of mountain ranges in the southern part of New Mexico. This unit consists of carbonate-cemented, burrowed, coarse granule sandstone that passes conformably basinward and upward into-burrow mottled, skeletal limestone and dolomite of the Upham Formation. The sandstone generally is massive and locally has large, straight *Skolithos* burrows that are up to .6 in wide, and up to 5 ft long. Locally cross-bedded in the Mud Spring and Caballos Mountains, this unit is interpreted to have formed as a large subtidal sandwave complex (Kelley and Silver, 1952; Bruno and Chafetz, 1988). Large *Maclurites* gastropods are the only fossil in this sandstone. At Rhodes Canyon, the Cable Canyon Sandstone is ~25 feet (8 m) thick.

Where the Cable Canyon Sandstone is absent the Upham Member, whose regional thickness is 40-140 feet (13-42 m), rests unconformably on the Early Ordovician El Paso Formation. The typical Upham Member is a light to dark colored, bioturbated skeletal dolomite. Fossils in the Upham Member include: *Maclurites*, brachiopods, crinoids, stromatoporoids, bryozoans, and corals. Phosphatized and iron-stained hardgrounds are abundant throughout this unit. These hardgrounds commonly are only traceable a few hundred meters or less. The Upham Member at Rhodes Canyon is ~85 ft (27 m) thick and capped by skeletal packstone containing numerous hardgrounds.

The Aleman Member, ~50-280 ft (16-85 m) thick regionally, conformably overlies the Upham Member and generally consists of a lower, dark gray calcisiltite interbedded with dark evenly bedded spiculitic chert that grades up into nodular, cherty skeletal dolostone. The Aleman Member in Rhodes Canyon is ~90 ft (28 m) thick and contains bryozoans and corals near its top.

The Cutter Member, 100-200 ft (30-60 m) thick regionally, conformably overlies the Aleman Member, and its lower part is composed of brown, massive, bioturbated shallow subtidal dolomite. The burrowed dolomite grades upward into interbedded burrowed dolomite and light colored, fine-grained tidal flat dolomite. The tidal flat dolomite contains cryptalgal laminites, mudcracks, spar-filled fenestrae and chert nodules after evaporites. The Cutter Member is capped by a regional disconformity overlain by the middle Early Silurian Fusselman Dolomite or Devonian Percha Shale. This unconformity varies regionally from a sharp planar surface to an irregular karsted surface underlain by sinkholes filled with Fusselman dolomite or younger clasts.

30.4/76.3 Note Bliss Formation and El Paso Group in roadcuts on right. (0.8)

31.2/75.5 Roadcuts in Bliss Formation on right. **(0.4)**

31.6/75.1 Cross arroyo floor. Granite Canyon to left. El Paso Group outcrops on right. Note old road bed at 2:00 along the base of the canyon wall. **(0.5)**

32.1/74.6 **STOP 2.** Stop at junction of Rhodes Canyon gravel road and the gravel road going north, up Bear Den Canyon. The very high ridge to the left, on the skyline, is Hardscrabble Mountain; it is capped by the basal limestone of the Lower Permian Hueco Group. Bear Den Canyon, to the right, represents the trace of the Bear Den Canyon Fault Zone, the object of this stop.

The Bear Den Canyon Fault is one of the main fault zones in the San Andres that appears to cause the mountain range to "bend" northeast (Fig. 2.8). It may mark the initiation of accommodation from the San Andres to the Sierra Oscura that we observed directly in Mockingbird Gap yesterday. Displacement is best seen on the left

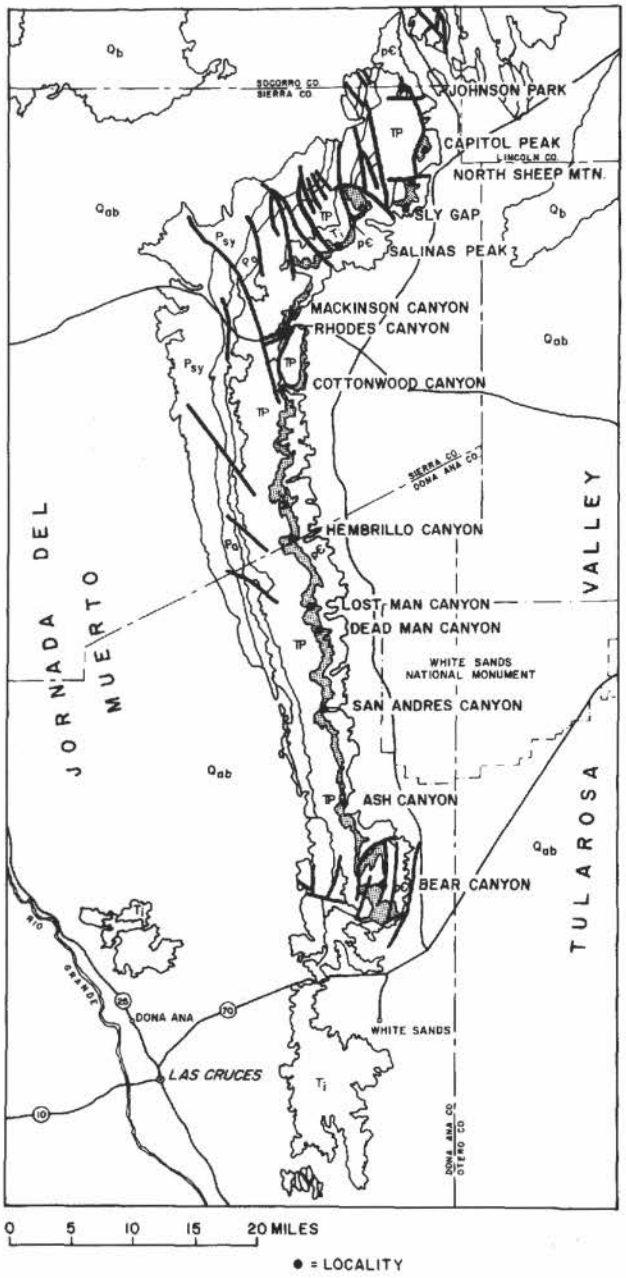

FIGURE 2.8. Generalized geologic map of the San Andres Mountains (modified from Sorauf, 1984). Map symbols are as follows: Qb = Quaternary basalt, Qab = Quaternary alluvium and bolson, Ti = Tertiary intrusives, Psy = Permian San Andres and Yeso Formations, Pa = Permian Abo Formation, IP = Pennsylvanian, pC = Precambrian. Stippled outcrop belt is rock of Cambrian through Mississippian age. Thick black lines are faults; thinner lines are contacts.

hand (western) side of Bear Den Canyon when looking north and places Ordovician Montoya Formation against Mississippian Lake Valley Formation (Tierra Blanca Member). The Tierra Blanca Member forms a thick ledge of crinoidal limestone bearing the characteristic white chert nodules of the member. The Rhodes Canyon road makes a sharp right angle bend here to the south were it roughly parallels the main fault. The arroyo paralleling the road contains a series of upthrown blocks of the Montoya Formation and the Bliss Sandstone (?) or clastic units in the Percha Shale, separated by anastomosing fault splays.

At the next right angle bend of the road (about 0.5 miles) the road leaves the trace of the fault and continues westward up Rhodes Canyon. At the second bend of the road the Bear Den Canyon fault is well exposed in the cutbanks on the southern side of the arroyo. Here, Montoya (?) carbonate beds on the east are upthrown against Upper Devonian (?) or Lower Mississippian (?) interbedded crinoidal limestone and black shale that display large drag folds. The limestone beds contain an abundant and diverse crinoid and brachiopod fauna.

Bear Den Canyon fault is mapped as a normal fault (Kelley, 1955) based on regional stratal age relationships adjacent to the fault. However, the exposed age relationships of the fault along this segment, display reverse motion (Fig. 2.9). Obviously, the age(s?) of the fault and tectonic setting(s?) have not been well established.

After stop, continue on unpaved road up Rhodes Canyon. **(0.5)**

32.6/74.1 Right turn in road. Bear Den Canyon Fault with drag folds to left (Fig. 2.10). Lead Camp Limestone outcrops straight ahead. **(0.1)**

32.7/74.0 Road continues to climb section to Lead Camp Limestone, which is well exposed to the right. **(0.4)**

33.1/73.6 **STOP 3**. Exposed along the road and within the arroyo are 622 ft (Kottlowski et al., 1956) of light to medium gray, thick to massive, cherty limestone beds intercalated with black calcareous shale of the Middle Pennsylvanian, Desmoinesian part of the Lead Camp Limestone (Fig. 2.11). The prominent limestone ledges and cliffs

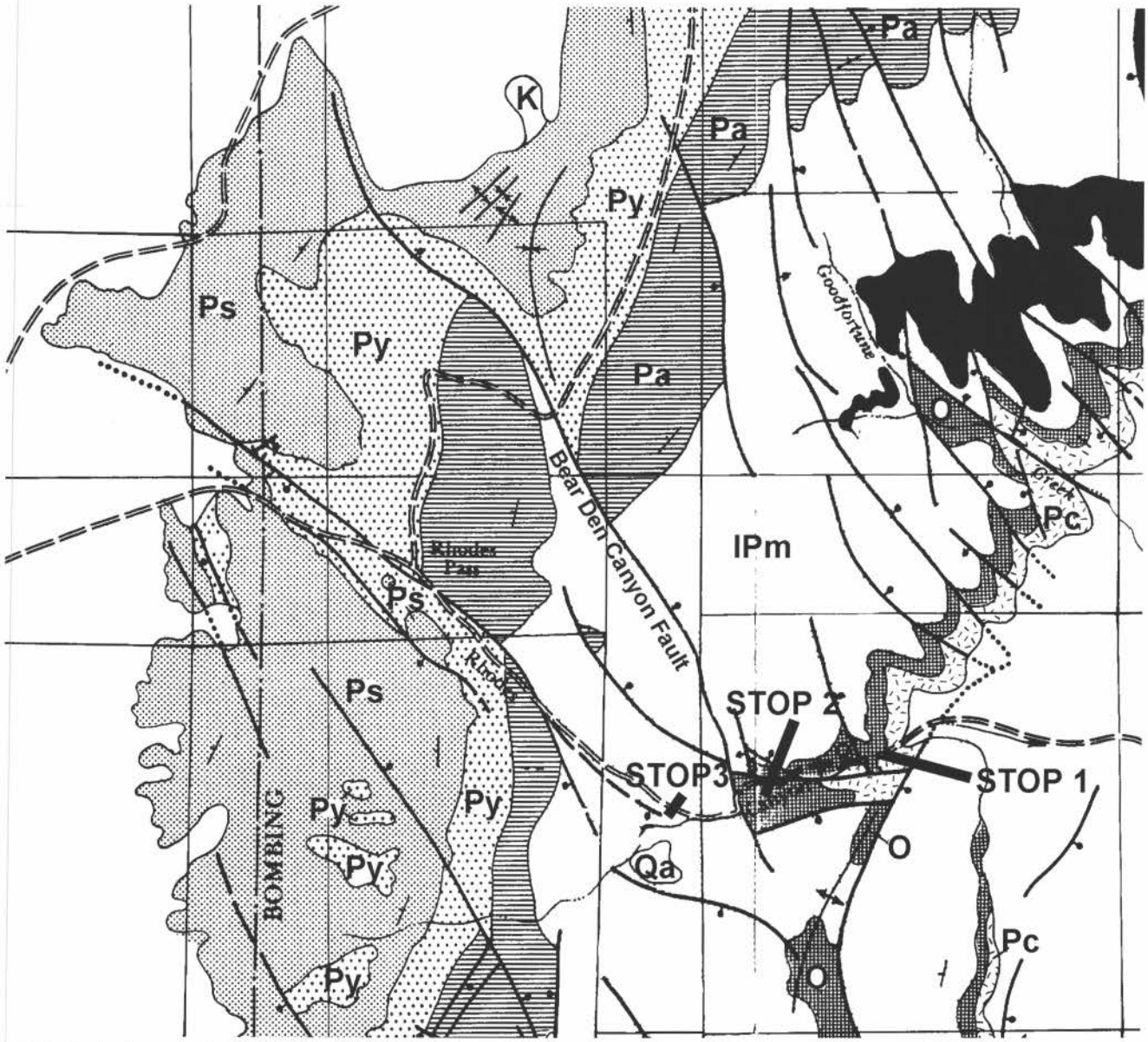

FIGURE 2.9. Geologic map of Rhodes Canyon in the vicinity of Bear Dean Canyon (modified from Kelley, 1955). Map symbols are as follows: K = Cretaceous Formations, Ps = San Andres Formation, Py = Yeso Formation, Pa = Abo Formation, C = Mississippian and Devonian Formations, O = Ordovician and Cambrian Formations, Pc = Precambrian. Black unit in northeast portion of the map is the intrusive sill at Salina Peak. Dark lines are faults with stick and ball on downthrown side.

are underlain by 230 ft of slope forming interbedded silty limestone, calcareous shale, siltstone, sandstone and conglomerate of the Atokan (Derryan) part of the Lead Camp. The Lead Camp Limestone correlates with the Gobbler Formation in the Sacramento Mountains, and the Desmoinesian limestone cliffs correlate with the Bug Scuffle Member of the Gobbler Formation. The Desmoinesian limestone cliffs at this stop contain an abundant and diverse marine fauna including *Fusulina, Eoschubertella, Wedekindellina, Pseudostafella* forams, brachiopods, echinoderms, and abundant *Chaetetes* sponges (Kottlowski et al., 1956). The Desmoinesian section is arranged into limestone/shale packages (cycles) that display systematic shifts stratigraphically upward in the ratio of limestone to shale within packages and depositional facies of the limestone ledges. The cycles stack into one third-order (1-10

FIGURE 2.10. Photograph of drag folds on the footwall of the Bear Den Canyon Fault.

my) transgressive-regressive sequence. The basal limestone cliff is the thickest and comprises very thick beds of bioturbated, fossiliferous inner to mid-shelf limestone containing interbedded glauconitic(?) calcareous sandstone beds near the base. The overlying thinner cliff is separated from the bottom cliff by an offshore shale unit. The second limestone cliff contains thick beds of mid-shelf fossiliferous limestone containing large "cannonball"-size chert nodules. The second cliff is overlain by a thick, shale-dominated recessive unit with thin ledges of middle to outer shelf fossiliferous limestone. This lower stack of limestone-shale cycles forms the transgressive part of the third-order sequence. Above the recessive shale unit the limestone ledges become progressively thicker and contain more shallow water facies, and the shale units become progressively thinner. The stacking pattern of the upper cycles forms the regressive part of the third-order sequence. After stop proceed on unpaved road up Rhodes Canyon. **(0.5)**

FIGURE 2.11. Photograph of the Lead Camp Limestone at Stop 3.

33.6/73.1 Road forks; **turn right**. Road to left goes up Bosque Canyon and continues to Sulfur Canyon. The road is on lower Panther Seep Formation, which forms canyon walls for next couple of miles. The Upper Pennsylvanian Panther Seep Formation of Kottlowski et al. (1956) is almost 1500 ft thick here and is mostly slope-forming olive-gray shale and thin beds of limestone, siltstone and sandstone. Some cliff forming algal bioherms ("patch reefs") also are present. Schoderbeck (1994) and Soreghan (1994) suggested that the Panther Seep reflects cyclical deposition driven by glacio-eustatic cyclicity. **(0.2)**

UPPER PENNSYLVANIAN SECTION IN RHODES CANYON

G.S. (Lynn) Soreghan
School of Geology and Geophysics, University of Oklahoma, Norman, OK 73019, lsoreg@ou.edu

Upper Pennsylvanian (Missourian-Virgilian) strata exposed within Rhodes Canyon comprise approximately 1400 ft of relatively shallow-water carbonate and siliciclastic facies deposited along the western margin of the late Paleozoic Orogrande basin. Most of this interval comprises the Panther Seep Formation, but the lower, carbonate-dominant part of the section (basal to middle Missourian) is part of the Lead Camp Limestone, which conformably underlies the Panther Seep Formation. The intercalated carbonate and siliciclastic motif continues into the Bursum Formation, which gradationally overlies the Panther Seep Formation. Several carbonate and siliciclastic facies types are present, and stack to form upwardly shoaling stratigraphic "cycles" ranging in thickness from approximately 15 to 250 ft.

Based on predominant lithofacies types and apparent cycle thicknesses, the Upper Pennsylvanian section in Rhodes Canyon comprises four, relatively distinct intervals, briefly described and interpreted below (Fig. 2.12). See Soreghan (1992, 1994a, b) for a more complete account of facies, cyclicity, and interpretations.

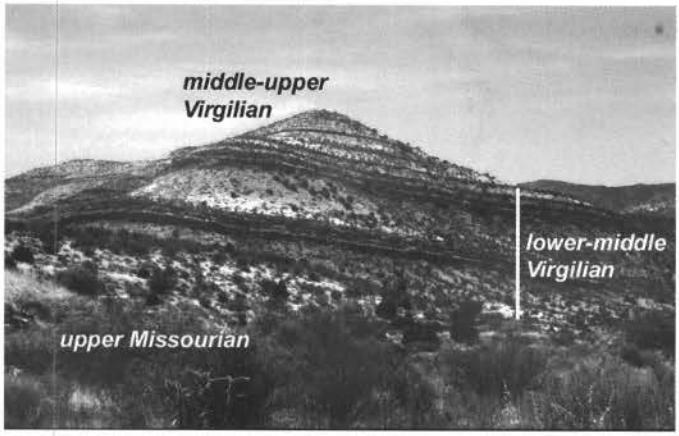

FIGURE 2.12. Photo looking west from near the junction of Rhodes and Bosque canyons, showing part of the Upper Pennsylvanian section. Visible in this view are (1) the poorly exposed upper Missourian section, which form the hillock in the foreground, (2) thick cycles of the lower-middle Virgilian section, and (3) middle-upper Virgilian section in the distant hill. (Photo modified from original photo taken by M. Elrick).

(1) The lower Missourian interval (approximately 200 ft thick) consists of normal marine carbonate with little to no siliciclastic material, and comprises the upper part of the Lead Camp Limestone. In this interval, repetitive cycles 30-40 ft thick consist of gray, normal marine "muddy" carbonate (fossiliferous wacke- and packstone) commonly grading upward to "grainy" carbonate (pack- and grainstone), with local development of incipient calcrete at cycle tops. This interval bears a close resemblance to the underlying Desmoinesian section of the Lead Camp Limestone, and records a continuance of the same conditions, i.e., a stable shallow-water carbonate shelf.

(2) The upper Missourian interval (approximately 150 ft thick) is poorly exposed in the hillock just west of the intersection of Rhodes and Bosque canyons, and consists of abundant, ledgey peritidal facies cyclically interbedded with very poorly exposed shale. Peritidal carbonates characteristic of this interval are commonly dolomitic, and contain abundant peloids and intraclasts, and relatively rare, euryhaline biota such as ostracodes, gastropods, foraminifers, and pelecypods. The change to these relatively thin (15-30 ft) cycles characterized by clearly restricted carbonate facies, and fine-grained shale, denotes a fundamental shift in conditions in the Orogrande basin, and marks the lower part of the Panther Seep Formation.

(3) The lower-middle Virgilian (approximately 675 ft) section records the first consistent appearance of arkosic siliciclastic facies, regularly intercalated with (typically) normal-marine carbonate in cycles ranging up to 250 ft thick. The siliciclastic component of cycles in this interval commonly comprises a coarsening-upward interval of micaceous mudstone, and fine- to coarse-grained arkosic sandstone displaying a variety of structures including planar, swaley, or cross-laminations, and local slumping within tabular to lenticular units. Within some particularly thick cycles in this interval, the siliciclastic component consists of a thick, monotonous dark mudstone. These facies appear to record deposition in a variety of fluvio-deltaic sub-environments, including delta front, bar, and interdistributary bay. The carbonate is typically normal marine, clean wackestone to pack- and grainstone that exhibits shallowing-up trends and exposure surfaces (calcrete) at cycle tops. The shift in facies types and thicknesses in this interval, particularly marked by the onset of basement-derived siliciclastic material, presumably reflects an episode of foundering and relatively rapid subsidence of the Orogrande basin with associated uplift of basement-cored sources (e.g., the Pedernal highland). The concurrence of both thick and shallow-water facies records rapid and paced sedimentation and accommodation. Notably, the correlative interval (middle Virgilian) elsewhere in the Orogrande basin also records a significant pulse of subsidence. In Hembrillo Canyon (San Andres Mountains), for example, algal bioherms with exceptionally thick, aggradational cycles occur in the middle Virgilian part of the section (sequences 5-6 of fig. in Soreghan and Giles, 1999a). In Dry Canyon (Sacramento Mountains), marked development of algal bioherms occurred in the middle Virgilian (e.g., Toomey et al., 1977), possibly reflecting maximum shelf accommodation during this apparent pulse of subsidence in the basin (cf. Soreghan and Giles, 2000).

(4) The middle-upper Virgilian interval (approximately 360 ft to the base of strata bearing "Bursumian" fusulinids) consists of mixed siliciclastic (arkosic)-normal marine carbonate cycles similar to those below, but exhibiting more regular and predictable facies motifs and cycle thicknesses (25-50 ft). This same pattern of facies and cycles continues though the remaining Panther Seep Formation, an additional 350 ft to the basal Bursum Formation (as designated by Kottlowski et al., 1956), although fusulinids within this interval record a "Bursumian" age. Relative to the great thickness and facies variations in the subjacent interval, this interval records more stable but still accelerated conditions of subsidence in this part of the Orogrande basin.

Pervasive cyclicity of the Upper Pennsylvanian section here and elsewhere reflects global eustasy driven by waxing and waning of late Paleozoic glaciers. Local evidence for this conclusion includes the typically abrupt juxtaposition of shoaling and emergence features atop subtidal cycle tops, which reflects forced progradation and base level fall sufficiently rapid to thwart normal (autogenic) progradation (e.g., Soreghan, 1994a, b; Soreghan and Dickinson, 1994). Regionally, evidence from the Upper Pennsylvanian section in Hembrillo Canyon documents minimum magnitudes of glacioeustatic fall approaching at least 300 ft (Soreghan and Giles, 1999b), easily sufficient to cause emergence of the shallow-water facies composing the Rhodes Canyon cycles. On the regional to global scale, the cyclic motif of the upper Paleozoic in general has been linked to glacioeustasy in many other regions of North America and Eurasia (e.g., Veevers and Powell, 1987; Heckel, 1986; numerous other studies).

33.8/72.9 Cross arroyo floor of Rhodes Canyon. Van Devender and Toolin (1983) analyzed and radiocarbon dated 13 packrat middens from Rhodes Canyon, identifying 108 kinds of plants. Glacial (late Wisconsinan) samples indicate mixed conifer and pine forests, and there was an increase in desert

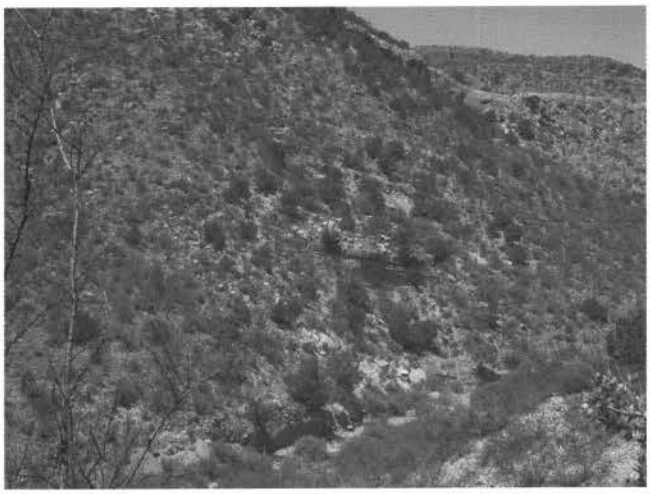

FIGURE 2.13. Photograph of Pennsylvanian-Permian transition at Stop 4.

and grassland species beginning about 9000 years ago. **(0.5)**

34.3/72.4 Old ranch house on right. **(0.6)**

34.9/71.8 Road passes through ledgy limestone beds of Panther Seep Formation. Thick white cliff of limestone on left ahead is the basal limestone of the Lower Hueco Group. **(0.2)**

35.1/71.6 Trees in the canyon below, left, mark location of Rhodes Spring. **(0.3)**

35.4/71.3 **STOP 4.** Examine Panther Seep to Hueco section on south side of road across canyon; Abo red beds ahead.

The section exposed on the canyon wall just south of the highway provides us an excellent chance to examine the Pennsylvanian-Permian transition in this region (Fig. 2.13). Lee (1909) and Darton (1928) first measured and mapped these strata, assigning the limestone-bearing strata (now Panther Seep and lower Hueco) to the Magdalena Group overlain by red-bed sandstones of the Abo Formation.

Thompson (1942, 1954) assigned the section to the Virgilian Fresnal Formation and Wolcampian Bursum Formation, Powwow Conglomerate, and Hueco Limestone. Kottlowski et al. (1956, fig. 8) termed it Virgilian Panther Seep Formation and Wolfcampian Bursum and Hueco formations. We assign it to the Panther Seep and Hueco formations (Fig. 2.14) and note the following:

The lower part of the section is olive-green shale interbedded with gray, blocky limestone, characteristic lithotypes of the Panther Seep Formation.

A striking, 10-ft thick bed of limestone-cobble conglomerate is the bed Thompson (1954) identified as Powwow Conglomerate and Kottlowski et al. (1956) marked as the base of the Bursum Formation. This bed, which may mark a sequence boundary, probably is correlative to the Bursum base father north.

However, the lithotypes of the overlying 200 ft or so of slope are not characteristic Bursum Formation lithotypes. The Bursum is readily identified by its interbedding of marine limestone and shale with nonmarine red-bed mudstones, sandstones and conglomerates (Lucas et al., 2000). No such nonmarine red beds are present here; instead, the slope is mostly beds of micaceous sandstone, drab shale and thin, nodular limestone, all characteristic Panther Seep lithotypes. Thus, although these strata indeed are correlative to Bursum strata to the north, on a purely lithostratigraphic basis they should be assigned here to the Panther Seep Formation.

A prominent, 25-ft thick limestone cliff is the base of the Hueco; it can be correlated to the south, where this limestone marks the base of the Hueco throughout the San Andres Mountains (Lucas et al., this guidebook). This cliff is mostly algal wackestones and lime mudstones with a prolific brachiopod fauna. Note the channel cut in a similar cliff of Hueco on the north side of the canyon (Fig. 2.15).

Above the cliff is a 1-2 ft thick limestone pebble conglomerate, which was the Hueco base of Kottlowski et al. (1956). It is overlain by red-beds and interbedded limestones. About 50 ft above the conglomerate we encounter the first fusulinids in the section, Wolfcampian *Schwagerina andresensis* Thompson.

So, where is the Pennsylvanian-Permian boundary in this section? It is definitely

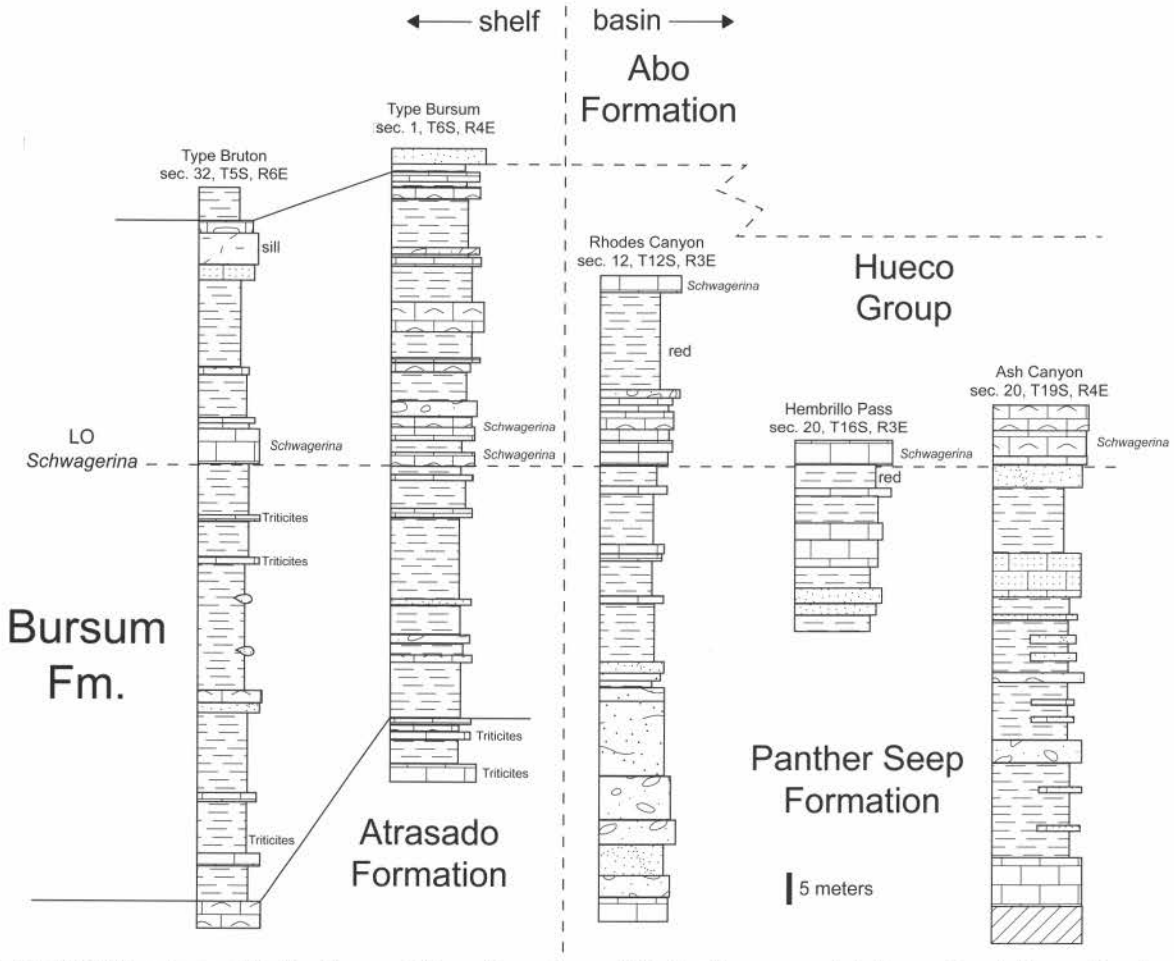

FIGURE 2.14. Stratigraphic column of Panther Seep and Hueco Formations at Rhodes Canyon correlated to sections to the north and south.

below the Hueco, which has Wolfcampian fusulinids to its base elsewhere in the San Andres Mountains. Presumably, the Wolfcampian base is somewhere in the upper Panther Seep, perhaps within the Bursum-equivalent interval, though it is impossible at present to put our finger on the exact boundary in this section.

After STOP continue west on the unpaved road. **(0.6)**

36.0/70.7 Panther Seep (olive colored shale and thin beds of limestone)—Hueco (thick gray limestone) contact on left. **(0.2)**

36.2/70.5 Cross creek. "Abo" red beds on the left actually have thin beds of marine (Hueco) limestone in them. Note coarse bouldery alluvium in creek bank is 20-30 ft thick. **(0.3)**

36.5/70.2 Cross creek again. Abo Formation to left of road. Faulting repeats section so that Hueco base is visible again as a cliff up the hill and to the right. **(0.4)**

36.9/69.8 Cross arroyo. Note Yeso Formation outcrops to left, on hill. **(0.2)**

37.1/69.6 Crest hill; road to left; at 10:00 Grandaddy Peak is a knob of San Andres Formation; Big Gyp Mountain at 12:00 (Fig. 2.16). **(0.4)**

37.5/69.2 Cross arroyo. **(1.1)**

38.6/68.1 Crest of hill; Big Gyp Mountain at 2:00 is Permian San Andres Formation over Yeso strata. **(0.7)**

39.3/67.4 Rhodes Pass, old Miller Ranch headquarters on left (Fig. 2.17). Turn around to retrace route down Rhodes Canyon to pavement. On the way down the canyon, note the workmanship displayed in the many rock walls that were built along old New Mexico Highway 51. (Fig. 2.18). **(5.3)**

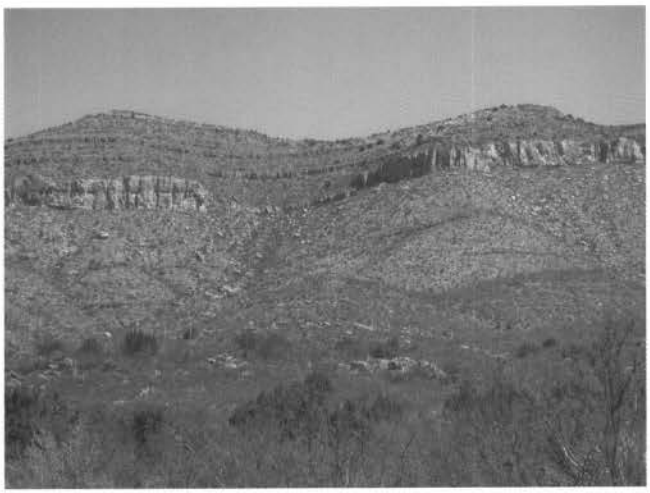

FIGURE 2.15. Channel cut in Hueco Group.

FIGURE 2.17. Miller Ranch Headquarters.

44.6/62.1 Road to right; note white Hueco limestone capping peak at 2:30; pass down into Lead Camp Limestone. **(7.8)**

52.4/54.3 Guardhouse, pavement begins. **(4.1)**

56.5/50.2 Intersection with main, paved, north-south range road at Rhodes Canyon Range Center; **turn right** to go south. **(2.5)**

59.0/47.7 Road to right to Gunsight Peak and Cottonwood Canyon. The road is built on a thin veneer of alluvial sediments derived from the east flank of the San Andres Mountains. **(1.5)**

60.5/46.2 Paved road to left; **continue straight**. **(1.6)**

62.1/44.6 Road curves left. **(3.6)**

65.7/41.0 Road curves left, Sulphur Canyon to right. Note White Sands at 10:00 in the distance. Near the head of Sulphur Canyon are small deposits of fluorite and barite known as the American Fluorspar Group or Bornstadt Claims. Very large crystals of museum-quality, deep purple fluorite have been found in these deposits. The overall nature of the mineralization is similar to that observed yesterday at the Independence Group of mines in Mockingbird Gap and Hansonburg. **(1.0)**

66.7/40.0 The Alkali Flat to the left is bordered on the north by a 60-ft tall bluff that exposes gypsiferous strata of Pleistocene Lake Otero. Late Pleistocene mammals from these strata include mammoth, horse and camel of Rancholabrean age (Morgan and Lucas, this guidebook). Road will now drop down

FIGURE 2.16. Photograph of Big Gyp Mountain taken from Rhodes Pass.

FIGURE 2.18. Stonework along former New Mexico Highway 51.

to the level of the Alkali Flat. **(0.6)**

67.3/39.4 Road curves right. **(1.0)**

68.3/38.4 Road to Shot Launch site to right. Large peak to the right is Kaylor Mountain. Immediately north of Kaylor Mountain is Grandview Canyon (Fig. 2.19). Proterozoic rocks are host to ore deposits of bismuth and tungsten in the canyon. Mineralization is weak but widespread in small veins and shear zones at schist-granite contacts. The ore consists of bismuthinite, native bismuth, bismutite and scheelite in a gangue mineral assemblage of magnetite, quartz and calcite. Minor amounts of chalcopyrite are also present. Display quality specimens of bismutite and scheelite have been produced from these small deposits. **(1.2)**

69.5/37.2 Road cut in gypsiferous Otero Formation. **(1.6)**

71.1/35.6 Building on right. Road intersection; road to right to Hembrillo Canyon visible to right.

Hembrillo Canyon to the right leads to the Hembrillo Basin, where a section of Panther Seep Formation about 1800 ft thick is exposed and includes well-studied algal bioherms. It is also the site of the legendary Victorio Peak treasure. Victorio Peak is cut by a fault that supposedly leads to an abandoned cavern in which, in 1937, treasure hunter Doc Noss claimed to have found gold bars and other riches. Unfortunately, Doc tried to blast open the crack that lead to the cavern and instead blocked access to it with fallen blocks of dolomite.

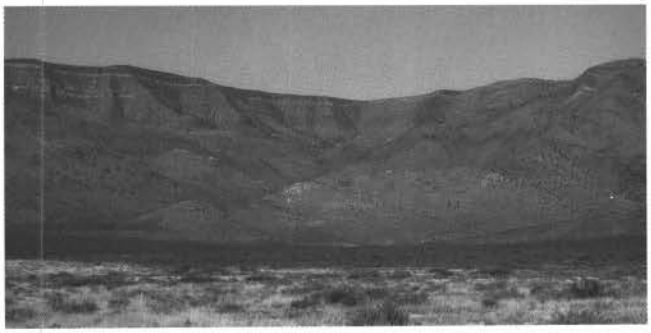

FIGURE 2.19. Photograph of Grandview Canyon.

FIGURE 2.20. Badlands formed in Lake Otero sediments.

Subsequent efforts to relocate the treasure have failed, and tales of Government conspiracy (some believe the Army took the treasure!) adorn this fable. **(0.2)**

71.3/35.4 Brillo Launch site to right; good view to left of Alkali Flat with Sacramento Mountains beyond to east (Fig. 2.20). The White Sands Space Harbor, a landing site for the space shuttle is to the east of here and accessed by the road to the left. **(2.1)**

73.4/33.3 **Stop 5. Pull off near culvert.** Here, we will examine gypsiferous strata of Pleistocene Lake Otero, their mollusc faunas (see Gordon et al. minipaper, this guidebook) and the fossil footprints exposed here. On the Alkali Flat to the left a surface covered with late Pleistocene mammoth and camel footprints (Fig. 2.21) has been known since the 1930s (see Lucas et al., this guidebook).

FIGURE 2.21. Mammoth footprints on Alkali Flat.

The Otero Formation is gypsiferous clay and sand, gypsite, and associated fluvial-deltaic facies deposited in and adjacent to Pleistocene Lake Otero in the Tularosa Basin. This lithostratigraphic unit, which excludes Holocene eolian and playa sediments of the White Sands-Lake Lucero-Alkali Flat area, forms much of the surficial basin fill here at elevations below 1,220m. The formation's areal extent is a least 2100 km^2. Originally named by C. L. Herrick in 1904, the term Otero Formation has never been used by subsequent workers. Further study, however, is needed to (1) decipher climatic and geomorphic history recorded by these lacustrine and fluvial-deltaic sediments, and (2) better define the formation's lateral and basal (subsurface) boundaries.

On the west side of the highway, note the Proterozoic structures well displayed in Hospital Canyon (Fig. 2.22). The structure within the entire mountain range at this location is a relatively simple monocline with some minor normal faults. (Fig. 2.23).

PLAYA LAKE SHORELINES AND THE HOLOCENE HISTORY OF THE WHITE SANDS DUNE FIELD

Richard P. Langford
Dept of Geological Sciences, University of Texas at El Paso, El Paso, Texas 79968-0555, USA, langford@geo.utep.edu

White Sands National Monument is the largest field of gypsum dunes in the world (Fig. 22.2). Recently, the importance of the deflation basin associated with the dunes has been emphasized (Fryberger, personal communication, 2000). In the central part of the Tularosa basin, deposition continued through the late Pleistocene and Holocene, where pluvial Lake Otero extended across the basin (Seager et al., 1987; Blair et al., 1990; Buck, 1996)). During the latest Pleistocene the penultimate shoreline formed at 1,216 m elevation (Seager et al., 1987). Shorelines formed at elevations of 1,210 and 1,207 m in isolated sub-basins of Lake Otero. Playa lakes, including Lake Lucero are incised into the sediments of Lake Otero. The dunes lie downwind of the playa and, between the dunes and the playa lakes lies the Alkali Flat, a desolate and largely unvegetated expanse of blowing gypsum sand within salt flats, and scattered Mesquite and Salt Brush.

An erosional shoreline surrounds modern Lake Lucero playa. This shoreline is partially buried beneath aggrading playa muds and salts, but forms a well-defined escarpment around all except the northern end of the playa. The base of this erosional shoreline escarpment is the nearly horizontal playa surface. Over fifty measurements give escarpment slopes of 30° to 40° in poorly consolidated Lake Otero sediments. Erosional shorelines are created by the erosive activity of waves when the playa is flooded. The base of erosional shoreline marks the level of flooding of the playa.

Two similar erosional shorelines can be correlated on the slopes above the modern playa. The lowest of the shorelines occurs at approximately 1,191 m elevation, approximately 5.5 meters above the surface of Lake Lucero. A second shoreline is located at approximately 1,200 m of elevation, 14.5 meters above the surface of Lake Lucero. These higher shorelines, mark elevations where playas formed between stages of deflation. The lower erosional shoreline (1191 m) is marked as the L-2 shoreline and the upper shoreline (1200 m), the L-1 shoreline. The L-2 shoreline is almost identical in morphology to the shoreline surrounding Lake Lucero. The upper, L-1 shoreline is a subtler feature that slopes 6° to 10° and is more gullied. Based on morphology the L-1 shoreline is older than the L-2 and Lake Lucero shorelines.

Erosion exposes older lacustrine sediments of Lake Otero in all of these shorelines at elevations below 1,215 m. Laminated carbonates and evaporites indicate deposition on the floor of a semi-permanent saline lake. Topographic profiles show the extent of deflation. Logged wells within the dunes indicate that the base of the eolian gypsum sand lies below the Lake Otero shoreline and slopes gently to the west. At the western edge of the dune field, the older lake muds are exposed, just above the L1 shoreline.

The horizontal beds of lacustrine Lake Otero sediments are essential to understanding the history of the White Sands because they define a low-relief Pleistocene lake floor. Thus, the topography of the basin below the Lake Otero Shorelines is largely a product of Post-Otero erosion. Because the shorelines are preserved, deflation has deepened the basin, but not widened it. Most previous authors have noted that two sources of gypsum dune sand, Otero Sediments and Lake Lucero (Allmendinger, 1971; LeMone, 1987). Allmendinger (1972) described a gypsum crystal-bearing layer in alkali flat up to 9m above the surface of Lake Lucero and suggested that deflation of these Pleistocene sediments produced most of the dunes. The main mass of the White Sands dune field begins abruptly near the L1 shoreline. However, several patches of parabolic dunes are forming by deflation of Lake Lucero and extend downwind from lake Lucero, partially burying the L1 and L2 shorelines.

Samples of eolian sand collected along a transect from the edge of the dune field indicating that the source of the White Sands is probably the older lake sediments below the L1 shoreline. Because the gypsum-bearing interval lies below the L1 shoreline, it is unlikely that a large dune field had formed until the deflation event between the L1 and L2 shorelines. No datable materials have been found yet on the L1 shoreline. However, searches of the archeological database at White Sands National Monument shows Folsom culture sites above the elevation of the L1 shoreline, but not within the L1 deflation basin (Eidenbach, Personal Communication, 2000). This suggests that the L1 shoreline can be dated

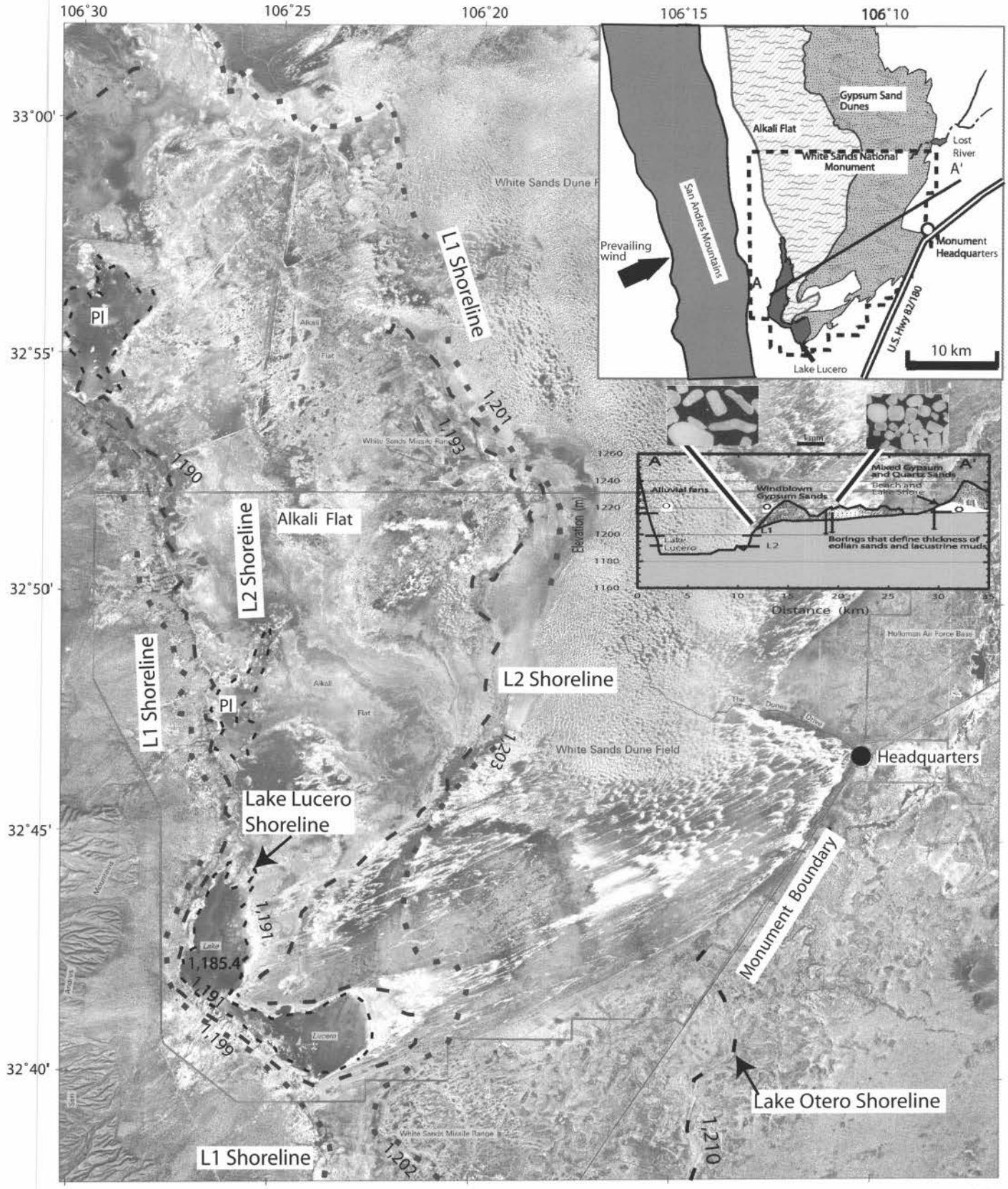

FIGURE 2.22 - Composite aerial photograph of Lake Lucero and the White Sands dune field. Dashed lines show erosional escarpments of the of Lake Lucero, L2, and L1 shorelines. Part of a depositional Lake Otero shoreline is evident to the southeast. Posted elevations mark sites of GPS measurements of shoreline elevation. (Aerial photograph supplied by White Sands National Monument and prepared by ESRI, Albuquerque, NM). Inset—Location map showing the relationship of the gypsum dunes to Lake Lucero and the alkali flat. Cross section A to A' shows the elevations of the Lake Lucero, the L 1 and L 2 shorelines and the Lake Otero shoreline.

FIGURE 2.23. Complex structures in Proterozoic rocks exposed at Hospital Canyon.

to younger than the 9,800 to 10,800 BP range of Folsom activity (Ingbar, 1992). (Local Folsom sites are widely scattered and their absence below the L1 shoreline may be due to other factors.)

Deflation of the L2 and Lake Lucero basins occurred after the establishment of a playa lake at the L1 level. Radiocarbon dates collected from the sediments below Lost River playa provided dates of 1,750 and 5,840 years BP (Monger and Gallegos, 1997). The dated sediments filled a basin dammed by the dunes suggesting that the growth of the White Sands dune field, and incision to the L2 shoreline occurred after 9,000 and before 5,840 BP. Two deflation events, dated at 7,000 and 4,000 yr b.p. are increasingly identified with playa basin and eolian sand generation in the region (e.g. Allen, 1991; Buck 1996).

The shoreline history described above implies, that while today, the dune field is actively migrating and is receiving a limited sand supply from the Alkali Flat, the majority of the growth of the White Sands dune field must have occurred during three short-lived arid climatic events, when the deflation basin was being deepened. One probably predated the dune field and occurred at the end of the Pleistocene resulting in deflation to the L1 shoreline. Two more events, the earliest circa 7,000 years BP formed the dune field and deflated to the L2 and Lake Lucero shorelines.

Dr. Steve Fryberger provided the impetus for this paper. The park staff at White Sands National Monument has been unfailingly helpful, particularly Dennis Vasquez and Bill Conrod.

The maximum size of Pleistocene Lake Otero estimated by Lucas and Hawley (this volume: area-2100 km^2) suggests a freshwater environment. In his original paper describing Lake Otero, Herrick (1904, p. 187-188) noted "The presence over its [Tularosa Formation] entire extent of recent fresh-water shells serves to indicate a comparatively fresh condition of the waters...." The presence of 25 species of freshwater and terrestrial mollusks, particularly relatively stenohaline taxa (e.g., *Stagnicola* spp. and *Pisidium casertanum*), confirm this hypothesis. However, all of the aquatic species present (including extant species such as the endemic hydrobiid snails and pupfish, *Cyprinodon tularosa*) or their progeniters originally may have colonized the lake passively via various vectors (e.g., mud attached to the legs of aquatic or shore birds). Hawley's (1993) contention that Lake Otero was restricted to the endorheic Tularosa Basin with no overflow into the Rio Grande drainage system appears to be valid.

Subsequent evaporation resulted in hyperhaline conditions, gypsum deposition, and the extirpation of the majority of the molluscan fauna. Relictual populations persist in a few permanent spring systems within Lake Otero's former drainage basin. The narrowly endemic aquatic species restricted to the Tularosa Basin help to reflect the age of formerly permanent aquatic systems in the Lake Otero drainage.

The paleoecology reflected by the composition of the mollusk community suggests lacustrine environments with shallow, nearshore freshwater habitats. Presence of large populations of planorbids, particularly *Gyraulus* spp., indicates the occurrence of nearshore macrophyte beds. The *Stagnicola* spp. are diagnostic of cool water habitats, paralleling the lower general temperatures during the late Pleistocene. Recent regional populations of these two lymnaeid species now are restricted to permanent water bodies in higher mountains (*S. elodes*) or highly fragmented populations in some cold springs at lower elevations (*S. caperata*) (MEG personal observations). Muddy margins without salt or gypsum deposition and with grassy shores surrounding the lake and lower reaches of tributaries are indicated by the large numbers of succineids and some pupillids (e.g., *Pupilla blandi*). Local species richness and particularly the occurrence of slugs (*Deroceras* sp.) noted in our study and Ashbaugh and Metcalf (1986) reflect a relatively mesic environment. Habitats occupied by *Gastrocopta cristata* suggest the presence of floodplain and stands of cottonwood (Metcalf and Smartt, 1997). Other species (e.g., *Vertigo ovata*) confirm the existence of woody, broadleaf plant communities and the presence of damp soil. Thus, at the time of deposition of these molluscan fossils, Lake Otero appears to have existed during a cool, mesic period of the late Pleistocene. It was a large, presumably deep, freshwater environment and located in an endorheic basin. Lake Otero generally possessed a floodplain and was surrounded by low-profile shores with muddy, grassy margins interspersed with stands of cottonwood and other communities of woody, broadleafed vegetation.

FOSSIL MOLLUSCAN FAUNA FROM PLEISTOCENE LAKE OTERO, TULAROSA BASIN, SOUTHERN NEW MEXICO

Mark E. Gordon, Gary S. Morgan, and Spencer G. Lucas
New Mexico Museum of Natural History, 1801 Mountain Rd., NW, Albuquerque, NM 87104

Pleistocene Lake Otero is located in the Tularosa Basin on the White Sands Missile Range (WSMR), northeastern Doña Ana County, southeastern Sierra County, and much of Otero County, southern New Mexico. The present playa, Lake Lucero, occupies part of Pleistocene Lake Otero's former bed. No species of mollusks have been identified previously from Pleistocene Lake Otero, but Herrick (1904, p. 179-180) did mention the presence of "...fresh-water lacustrine shells" in his Tularosa Formation or "Tularosa Beds" (considered the upper portion of the Otero Formation by Lucas and Hawley, this volume). In September

2000, Robert Myers, a geologist at WSMR, discovered fossils in the Otero Formation on the WSMR just north of White Sands National Monument. Myers screenwashed a small sediment sample from this site and recovered numerous mollusks and several small vertebrates. Morgan and Lucas visited WSMR in December 2001 and January 2002 and collected additional sediment samples for screenwashing from Myers' site and three other sites in the Otero Formation. All four sites yielded mollusk fossils. A few km east of the WSMR boundary near Oscuro, southwestern Lincoln County, Ashbaugh and Metcalf (1986) reported 38 taxa identified to species of Pleistocene mollusks from five localities in the dry arroyo downstream from Keen Spring. The Keen Spring sites are in the Tularosa Basin but are in sediments deposited outside the limits of Pleistocene Lake Otero (Herrick, 1904; Hawley, 1993; Lucas and Hawley, this volume).

Most of the molluscan fossils reported here were collected at New Mexico Museum of Natural History (NMMNH) site L-4980 in upper Pleistocene lacustrine sediments on the western edge of the Alkali Flat, northwestern Doña Ana County, ~0.5 km northwest of the mammoth track site (L-4979; see Lucas et al., this volume). Numerous fossil Ostracoda were also recovered from this site and L-4981 but were not identified for this study. The fossils occur in a green gypsiferous clay (unit 6; see stratigraphic section in Lucas et al., this volume) less than 0.5 m thick and about 1.0-1.5 m above the floor of a fairly deep, narrow arroyo. Several thousand individuals representing 22 species of mollusks (Table 1) were identified from a 200 kg sample of sediment that we collected and screenwashed. Ten species of vertebrates, mostly small species (e.g., frogs, snakes, and rodents: see Morgan and Lucas, this volume), also were identified from this sediment sample. The molluscan faunas from the other three sites are much less diverse, ranging from four to ten species (Table 1); however, the sediment samples washed from these sites also were much smaller. Site L-4981 is 0.5 km south of L-4980 and is derived from unit 4,~1 m lower in the stratigraphic section and just above the unit that contains the mammoth tracks. A 10 kg sediment sample from L-4981 consisted of a light-colored, greenish-gray clay and yielded six species of mollusks (Table 1). Sites L-4984 and L-4985 are located ~10 km due north of L-4980 and L-4981 in a series of badlands that form a prominent southwest-northeast-trending escarpment. Both sites occur in claystones of the Otero Formation. A 1 kg sediment sample from L-4984, a reddish gypsiferous clay (unit 6; see stratigraphic section in Lucas and Hawley, this volume), yielded four species of mollusks (Table 1). A 10 kg sediment sample from L-4985, a mottled reddish/greenish gypsiferous clay (unit 12), located about 3 m ; see Lucas and Hawley, this volume), contained 10 species of mollusks (Table 1).

Robert Myers helped arrange access to the White Sands Missile Range and donated an important sample of fossil mollusks to the NMMNH. Pete Reser assisted in the field.

TABLE 1. Pleistocene molluscan fauna from the Otero Formation, White Sands Missile Range, Doña Ana and Sierra counties, New Mexico. "X" indicates presence; "—" indicates absence. For genera with more than one unidentified species (e.g., *Physa*), the number in parentheses after the X indicates the number of species in that genus present per locality.

Species	Localities			
	L-4980	l-4981	L-4984	L-4985
Gastropoda (terrestrial)				
Pupillidae				
Pupoides cf. *albilabris* (Adams 1841)	X	—	—	—
Pupilla blandi Morse 1865	X	—	—	—
Pupilla muscorum (Linnaeus 1758)	X	—	—	—
Gastrocopta cristata (Pilsbry & Vanatta 1900)	X	—	—	—
Gastrocopta pellucida (Pfeiffer 1841)[1]	X	—	—	—
Vertigo ovata (Say 1822)	X	—	—	—
Valloniidae				
Vallonia perspectiva Sterki 1893	X	—	—	—
Succineidae				
Catinella spp. (at least 2 species)	X (2)	X	—	—
Succinea spp. (at least 3 species)	X (2)	X	[2]	—
Oxyloma spp (probably 2 species)	X (2)	—	—	—
Limacidae				
Deroceras sp.	X	—	—	X
Gastropoda (aquatic)				
Lymnaeidae				
Stagnicola elodes (Say 1821)	X	—	—	X
Stagnicola caperata (Say 1829)	X	X	—	X
Physidae				
Physa spp. (at least 3 species)	X (3)	X (3)	X (2)	X (3)
Planorbidae				
Gyraulus circumstriatus (Tryon 1866)	X	—	—	X
Gyraulus cf. *deflectus* (Say 1824)	X	—	—	X
Gyraulus parvus (Say 1817)	—	—	X	X
Planorbella tenue (Dunker 1850)	—	—	—	X
Bivalvia				
Sphaeriidae				
Pisidium casertanum (Poli 1791)	X	—	—	—
Total number of species	22	6	4	10

[1]This is the *hordeacella* Pilsbry 1890 morph and may warrant consideration as a distinct taxon.

[2] This represents an unidentifiable fragment of a juvenile succineid.

After the Stop, continue south on the paved road. **(0.6)**

74.0/32.7 Road curves left. **(0.4)**

74.4/32.3 Road curves left. **(1.8)**

76.2/30.5 Road curves left. **(0.4)**

76.6/30.1 Road curves right, radar installation on right. **(0.6)**

77.2/29.5 Chile launch site to left. **(0.5)**

77.7/29.0 Cross road; **continue straight**. Dead Man and Lost Man Canyons to right. Gardner Peak at 2:00. Copper vein deposits have been exploited from mines in San Andrecito, Deadman, Lostman and Hembrillo Canyons. The deposits consist of veins of chalcopyrite and chalcocite in a gangue of quartz, hematite, and calcite. The veins have been oxidized to cuprite and malachite in places. The veins are hosted in Bliss sandstone and Montoya group rocks.

All of the deposits are small and production has been scant. **(1.1)**

78.8/27.9 Vandal launch site on left. **(2.2)**

81.0/25.7 Rad launch site to right. Road to right to Mayberry Canyon on right at 2:30. **(1.3)**

82.3/24.4 Road curves left. **(0.4)**

82.7/24.0 Enter White Sands National Monument, Zone of Cooperative Use. **(0.4)**

83.1/23.6 Road jogs right. **(2.7)**

85.8/20.9 Road curves right. **(0.7)**

86.5/20.2 Road to right to San Andres Canyon which is at 3:00. Lake Lucero at 10:00 on left. The San Andres Lead Mine is located on the north side of San Andres canyon about a quarter of a mile west of the small missile range boundary. Similar to most deposits in the range it is a carbonate replacement type consisting of barite, quartz, and galena. The development on the ore deposit, including the building of a mill and smelter, was never justified considering the size and grade of the orebody. **(1.4)**

87.9/18.8 Lake Lucero on left. Lake Lucero is a playa lake plain on the remarkably flat floor of the Tularosa Basin (Fig. 2.24). When fully flooded, the lake has covered as much as 8.5 mi^2 (in 1942). However, its late Pleistocene (Wisconsinan) predecessor, Lake Otero, has relict shorelines and gypsum deposits that suggest that during pluvial conditions it covered at least 700 mi^2 (Herick, 1904; Hawley and Kottlowski, 1969; Lucas and Hawley, this guidebook). **(2.5)**

QUATERNARY FLOODING OF THE TULAROSA BASIN? — IMPLICATIONS OF A SOIL-WATER-CHLORIDE PROFILE FROM WSMR

William J. Stone
Earth & Environmental Sciences Division,
Los Alamos National Laboratory, MS T003, NM 87545

White Sands Missile Range (WSMR) lies in the Tularosa Basin, a typical Southwestern alluvial basin, situated between the Organ Mountains on the west and the Sacramento Mountains

FIGURE 2.24. Geologic cross-section near this locality from Darton (1928).

on the east. The U.S. Army operated a hazardous-waste-disposal facility 10 mi east of the WSMR headquarters in the period 1977-1981. In response to concern over the potential for migration of contaminant from the facility to area water-supply wells, the U.S. Geological Survey was contracted to make a hydrogeologic study of the site in 1988. The then New Mexico Bureau of Mines and Mineral Resources was sub-contracted to conduct a chloride-mass-balance/recharge study of the upper part of the unsaturated zone beneath the facility (Stone, 1988). Although soil-water flux was calculated in the 1988 study, soil-water age at the site was not addressed. The purposes of this minipaper are to re-examine the chloride profile obtained in that study and its implications for pluvial conditions in the Tularosa Basin.

The surface at the facility is characterized by the Dune Land/Doña Ana soil complex, which is classified as highly permeable (Neher and Bailey, 1976). The facility is underlain by typical basin-fill deposits of Quaternary age: interbedded sand, silt, and clay. In 1986, ground water depth ranged from 229 to 236 ft in three test wells at the facility (Myers and Pinckley, 1987). Lab analysis of core obtained by hollow-stem augering yielded a geologic log as well as profiles for moisture and soil-water-chloride content (Fig. 2.25). Data from these were used to estimate the long-term average soil-water flux (F_{sw}) at the site, using average annual precipitation (P), total chloride input to the site from precipitation and dust (Cl_t), and average chloride content of soil water (Cl_{sw}): $F_{sw} = (PCl_t)/Cl_{sw}$ (Stone, 1992a).

As is often the case, on-site values for P and Cl_t were not available. However, data for P were available from nearby White Sands National Monument. Based on 22 yrs of record, the average annual precipitation there is 7.61 inches. The closest station where Cl_t has been determined is Mayhill, New Mexico. A value of 0.286 mg/L was reported for Mayhill by the National Atmospheric Deposition Program (1988a,b). Using these values and 218 mg/L for Cl_{sw} from analysis of core gives an average soil-water flux of 0.01 in/yr.

Soil-water chloride profiles normally have just a single peak or bulge near the surface. Such peaks develop in the root zone because plants selectively take up water but not salt (Stone, 1992b). Interestingly, the WSMR profile is characterized by two chloride peaks (Fig. 2.25). The interval of low soil-water-chloride content between the peaks at WS-1 represents a marked change in soil-water conditions. Such a change was apparently characterized by less plant activity, increased recharge or both.

The most likely scenario for the origin of this profile is that the lower peak formed at the surface in the usual way, but was then displaced downward (by piston flow) as the result of several events:

1. The lower chloride bulge developed in the root zone near the ground surface.

2. Flooding in at least this portion of the Tularosa Basin killed off the plants responsible for the accumulation of chloride in the profile.

3. The influx of fresher surface water to the unsaturated zone led to downward flushing of the chloride bulge.

4. The standing water eventually receded and dried up.

5. When plant cover was re-established, the upper chloride bulge formed.

The profile thus has two peaks separated by an interval of low soil-water chloride.

Presumably, such flooding occurred under pluvial conditions in the Pleistocene. But, can soil water be dated and if so, does the age of the freshening of the chloride profile support such an interpretation? Cumulative soil-water-chloride content above a given point in a profile (Cl_{cum}) has been used to approximately date soil water at that point (Allison and others, 1985; Stone, 1992b). More specifically, age (A) in years before present (BP) can be approximated using Cl_{cum}, P and Cl_t, as defined above:

$$A = Cl_{cum}/(PCl_t).$$

Using Cl_{cum} at the base of the low chloride interval (11,394 mg/L) and values for P and Cl_t as given above, yields an approximate age for the freshening or flooding of 14,500 yrs BP. Such an age clearly falls within the Pleistocene. More significantly, the age falls between 25,000 yrs BP, the onset of the late Wisconsinan lacustral interval (Morrison and Frye, 1965), and 11,000 yrs BP, the end of the Pleistocene. It also compares fairly well with the age of ancient Lake Animas, a well-studied pluvial feature at a similar latitude in Hidalgo County, New Mexico. Three stages of still-stand, represented by three distinct shoreline ridges around the edges of the lower Animas Valley, characterized Lake Animas. Several lines of evidence support a Holocene age for the lower and intermediate shorelines. However, the early phase of Lake Animas was assigned a general age of late Wisconsinan, based on geomorphic relationships and soil characteristics for the highest shoreline, (Fleischhauer and Stone, 1982). More specifically, the earliest phase of the lake occurred at least 11,000 yrs BP, based on the ages of the disappearance of piñon from Southwestern basins and lake maxima in the Great Basin.

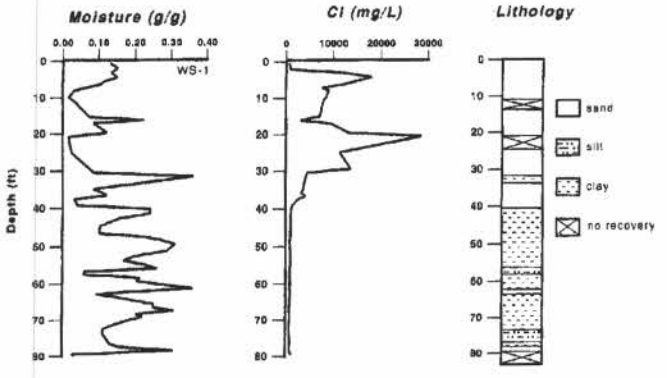

FIGURE 2.25 Moisture-content profile, soil-water-chloride profile, and geologic log for White Sands Missile Range hole WS-1 (modified from Stone, 1992a, Figure 4).

As discussed by Stone (1988), soil-water fluxes determined by the mass-balance method are only as good as the values used for P and Cl_t. The same goes for the soil-water ages, determined as described here. The value used for P comes from a nearby station also on the Tularosa Basin floor and should be representative. However, the value used for Cl_t comes from a station in a different setting (Mayhill). P at Mayhill is more than twice that in the Tularosa Basin, due no doubt to its location on the rainy side of the Sacramento Mountains. Intuitively, if P is greater at Mayhill than in the Tularosa Basin, Cl_t should also be greater than in the Tularosa Basin. In fact, however, Cl_t values are of the same order of magnitude across New Mexico, regardless of setting or elevation. For example, Cl_t at the Sevilleta Refuge north of Socorro, New Mexico, is 0.37 mg/L as compared to 0.29 mg/L at Mayhill. Therefore, the soil-water flux and age determinations at the WSMR site are probably reasonable, even though on-site values were not available for key parameters.

To conclude, the WSMR chloride profile provides interesting insight into changes that may have occurred during the Quaternary in Southwestern alluvial basins in general and in the Tularosa Basin in particular.

90.4/16.3 Road to right. San Andres Peak to right (Fig. 2.26). This section of the range is relatively uninterrupted by faulting (Fig. 2.27). **(1.0)**

91.4/15.3 Road curves left; leaving White Sands National Monument. **(0.7)**

92.1/14.6 Ash Canyon at 2:30. **(1.5)**

93.6/13.1 Road to right to Ash Canyon. **(2.5)**

96.1/10.6 Road curves right. **(1.3)**

FIGURE 2.26. San Andres Peak.

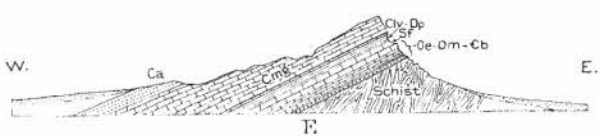

FIGURE 2.27. Geologic cross-section at San Andres Peak.

FIGURE 2.28. Photograph of the north side of Bear Canyon. Structures illustrated in Figure 2.29.

97.4/9.3 Road to Little San Nicolas Canyon to right; Goat Mountain at 2:00. **(1.6)**

99.0/7.7 Black stripe to right very low on the slope of Goat Mountain (just above alluvial fan surface) is Proterozoic amphibolite. **(2.7)**

101.7/5.0 Road to right to Bear Canyon at 3:00; Organs Mountains ahead at 1:00. Two groups of mines are found up Bear Canyon and two miles north to Lee Gulch that comprise the Bear Canyon mining district. One group of mines is along the foothills on the east side of the mountains, and the other is located near the crest of the range. Very small production has occurred from the deposits (Dunham, 1935). The deposits are predominantly carbonate replacement type, and the ore mineral assemblage consists of barite, galena, and fluorite. The deposits are most famous for the development of secondary minerals that include vanadinite and wulfenite **(3.8)**

This portion of the San Andres Range is highly deformed in comparison to regions immediately to the north (Fig. 2.28). Laramide thrusting and folding were identified by Seager (1981) in the area of Bear Peak. These Laramide structures were, in turn, faulted into segments, adding to the structural complexity of the area (Fig. 2.29)

105.5/1.2 Road curves left; San Agustin Pass at 2: 30. **(0.6)**

106.1/0.6 Tanks on left. **(0.5)**

106.6/0.1 Gate at entrance to Small Missile Range **(0.1)**

106.7/0.0 Junction US 70. Turn left, return to Alamogordo. See Day 3 guide.

End of Second-day Road Log.

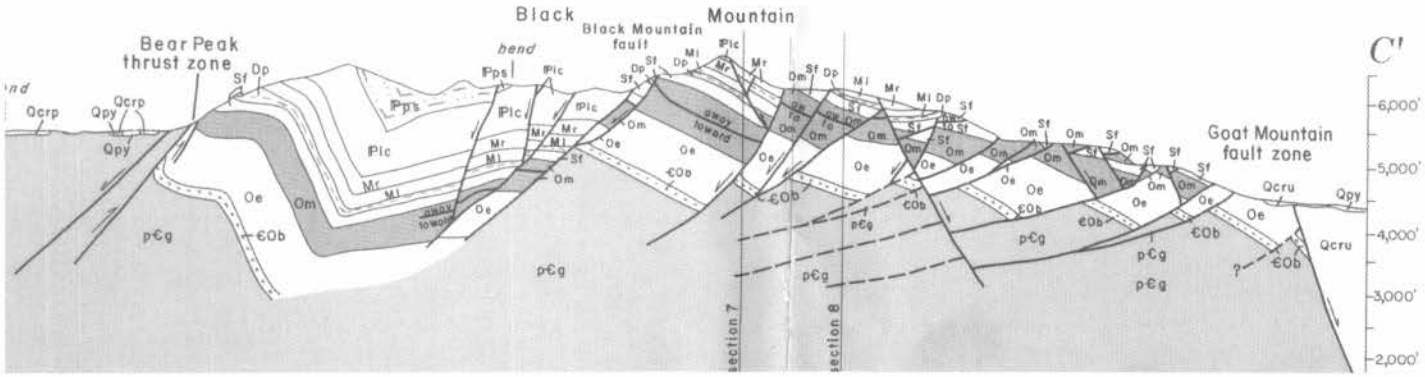

FIGURE 2.29. Geologic cross section near Bear Canyon by Seager (1981).

This paper was approved for public release by White Sands Missile Range; distribution unlimited. OPSEC review completed on June 25, 2002.

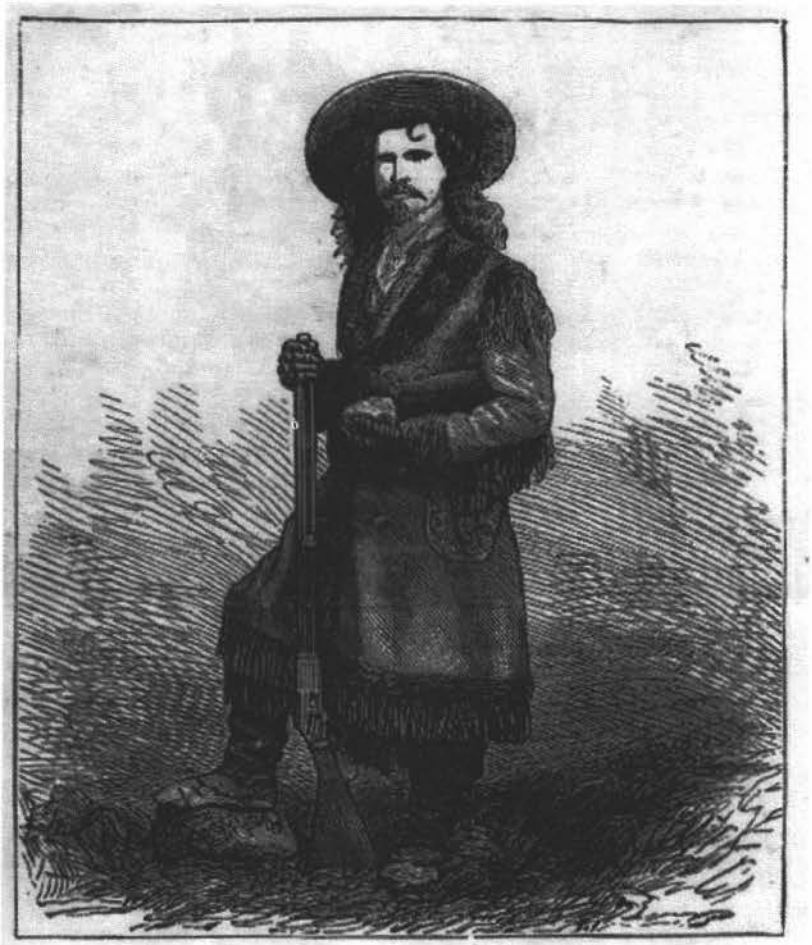

JACK CRAWFORD, INDIAN GUIDE AND SCOUT TO THE U.S. ARMY

Captain Jack Crawford (1847-1917), New Mexico's famed "Poet Scout" is remembered not only for his exemplary service as Chief of Scouts for the U. S. Military and many well-received books of prairie poetry, but he was also one of territorial New Mexico's more successful pioneer prospectors (see "Good Fortune" mini-paper, this guidebook). He is depicted in the above woodcut brandishing the tools of his trade: rifle in one hand and a chunk of high-grade ore in the other. Many of his contemporaries credit Crawford with almost single-handedly making the Magdalena, San Andres, and Black Range areas safe for prospectors (*The Graphic*, February 23, 1884 – Photo and caption courtesy of Robert W. Eveleth).